Pectin influences the kinetics of *in vitro* lipid digestion in oil-in-water emulsions

Verkempinck, S.H.E.[1*], Salvia-Trujillo, L.[1/2], Denis, S. [1], Van Loey, A.M.[1], Hendrickx, M.E.[1], Grauwet, T.[1]**

[1] Laboratory of Food Technology and Leuven Food Science and Nutrition Research Centre (LFoRCe), Department of Microbial and Molecular Systems (M^2S), KU Leuven, Kasteelpark Arenberg 22, PB 2457, 3001, Leuven, Belgium

[2] Food Technology Department, University of Lleida, Rovira Roure 191, 25198 Lleida, Spain

Running title:

Effect of pectin on lipolysis kinetics

Author's email addresses:

Verkempinck, S.H.E.: sarah.verkempinck@kuleuven.be

Salvia-Trujillo, L.: lsalvia@tecal.udl.cat

Denis, S.: denis.sofie@gmail.com

Van Loey, A.M.: ann.vanloey@kuleuven.be

Hendrickx, M.E.: marceg.hendrickx@kuleuven.be

Grauwet, T.: tara.grauwet@kuleuven.be

Journal: Food Chemistry

Submitted: February 2018

Resubmitted: April 2018

*author whom correspondence should be addressed during submission process:

sarah.verkempinck@kuleuven.be

+32 16 37 63 32

** author whom correspondence should be addressed post-publication:

tara.grauwet@kuleuven.be

+32 16 32 19 47

Abstract

Oil-in-water emulsions were prepared with 5% (w/v) carrot-enriched olive oil and stabilized with Tween 80 (TW), phosphatidylcholine (PC), citrus pectin (CP) or a combination of these emulsifiers. Additionally, the methylesterification degree (DM) of citrus pectin was modified, resulting in three different studied pectin structures: CP82, CP38 and CP10. All initial emulsions presented small initial oil droplet sizes and were submitted to an *in vitro* simulated gastric and small intestinal phase. The latter was executed in a kinetic way to determine the time dependency of the lipolysis reaction, micelle formation and carotenoid bioaccessibility. The results showed that the pectin DM mainly influenced the reaction rate constants, while the emulsifier (combination) determined the extent of lipolysis and carotenoid bioaccessibility. Moreover, a direct relation was observed between the lipolysis reaction and bioaccessibility extent. The presented study showed that targeted emulsion design can be used to tailor lipid digestion kinetics.

Keywords: citrus pectin; emulsion; *in vitro* digestion; lipolysis; carotenoids.

Chemical compounds: Tween 80 (PubChem CID: 5281955); Phosphatidylcholine (PubChem CID: 16219824); Lipase (PubChem CID: 54603431); Bile salt (PubChem CID: 439520); Calcium (PubChem CID: 5460341); α-carotene (PubChem CID: 4369188); β-carotene (PubChem CID: 5280489).

Abbreviation list:

BAC: bioaccessibility

CP: citrus pectin

CP82; CP38 or CP10: citrus pectin with a methylesterification degree of 82%, 38% and 10%, respectively

CP82 emulsion: 5% (w/v) olive oil-in-water emulsion stabilized with 1% (w/v) citrus pectin with a methylesterification degree of 82%

CP38 emulsion: 5% (w/v) olive oil-in-water emulsion stabilized with 1% (w/v) citrus pectin with a methylesterification degree of 38%

CP10 emulsion: 5% (w/v) olive oil-in-water emulsion stabilized with 1% (w/v) citrus pectin with a methylesterification degree of 10%

DAG: diacylglycerol

DM: methylesterification degree

FFA: free fatty acids

GLY: glycerol

HMP: high methoxylated pectin

JCR: joint confidence region

LMP: low methoxylated pectin

MAG: monoacylglycerol

MMP: medium methoxylated pectin

o/w emulsion: oil-in-water emulsion

PC: Phosphatidylcholine

PC emulsion: 5% (w/v) olive oil-in-water emulsion stabilized with 1% (w/v) phosphatidylcholine

PCCP82 emulsion: 5% (w/v) olive oil-in-water emulsion stabilized with 1% (w/v) phosphatidylcholine and 1% (w/v) citrus pectin with a methylesterification degree of 82%

PCCP38 emulsion: 5% (w/v) olive oil-in-water emulsion stabilized with 1% (w/v) phosphatidylcholine and 1% (w/v) citrus pectin with a methylesterification degree of 38%

PCCP10 emulsion: 5% (w/v) olive oil-in-water emulsion stabilized with 1% (w/v) phosphatidylcholine and 1% (w/v) citrus pectin with a methylesterification degree of 10%

TAG: triacylglycerol

TW: Tween 80

TW emulsion: 5% (w/v) olive oil-in-water emulsion stabilized with 0.5% (w/v) Tween 80

TWCP82 emulsion: 5% (w/v) olive oil-in-water emulsion stabilized with 0.5% (w/v) Tween 80 and 1% (w/v) citrus pectin with a methylesterification degree of 82%

TWCP38 emulsion: 5% (w/v) olive oil-in-water emulsion stabilized with 0.5% (w/v) Tween 80 and 1% (w/v) citrus pectin with a methylesterification degree of 38%

TWCP10 emulsion: 5% (w/v) olive oil-in-water emulsion stabilized with 0.5% (w/v) Tween 80 and 1% (w/v) citrus pectin with a methylesterification degree of 10%

1 Introduction

Lipids are the macronutrients with the highest energy density, which deliver essential fatty acids and can be carriers of lipophilic micronutrients, such as carotenoids (Golding & Wooster, 2010). In the human diet, lipids are frequently consumed as oil-in-water (o/w) emulsions, such as soups and sauces, being natural sources of fibers and micronutrients. Lipid digestion predominantly occurs in the small intestine, where triacylglycerol (TAG) can be hydrolyzed by pancreatic lipase into diacylglycerol (DAG), monoacylglycerol (MAG), free fatty acids (FFA) and glycerol (GLY). Subsequently, these lipid digestion products form mixed micelles together with bile salts excreted from the liver. These mixed micelles are amphiphilic structures which can incorporate lipophilic components in the core and easily migrate in the aqueous intestinal environment towards the intestinal mucosa (McClements & Decker, 2009). The fraction of ingested lipids and lipophilic components which are micellarized and consequently are available for absorption into the blood, is called the 'bioaccessible' fraction.

Recently, digestion studies were more focusing on controlling the lipid digestion rate as it plays an important role in satiety control, which in turn is related to food intake and diseases of nutritional excess (Ohlsson et al., 2014). Previous research has shown that dietary fibers, such as chitosan, cellulose, guar gum and pectin, may affect lipid digestion based on analysis of FFA release (Pasquier et al., 1996; Mun et al., 2006; Hur et al., 2013; Espinal-Ruiz et al., 2014a). It can be postulated that by increasing the intake of natural fibers, the lipid digestion mechanism can be modified and subsequently lipid intake can be controlled. In addition, lipid digestion is strongly related to the uptake of lipophilic carotenoids (Borel et al., 1996; Deming & Erdman, 1999), so modulating the lipolysis extent might also have influence carotenoid uptake. Therefore, the effect of the presence of fibers in food systems must be investigated on the kinetics of both lipid digestion as well as carotenoid bioaccessibility.

Pectin is one of the most abundant fibers present in the primary cell wall and middle lamella of all higher plants (Willats et al., 2001). It is a diverse group of polysaccharides rich in galacturonic acid (GalA) units which recently has shown emulsifying and emulsion-stabilizing potential (Schmidt, Schwab, & Schuchmann, 2017). Since pectin is a natural ingredient, it can be interesting to explore its role as emulsifier or when it is present in the aqueous phase of o/w emulsions on the lipolysis kinetics. It is known that the properties of the oil droplet, oil-water interface and surrounding medium can have a major effect on the lipolysis kinetics. In this context, it was proven that initial small oil droplet sizes led to a faster and higher lipolysis than larger initial oil droplets (Salvia-Trujillo et al., 2017). Not only initial small oil droplets are of importance, but also the stability of these oil droplets along the simulated digestive tract, which can be influenced by the emulsifier type used for emulsion stabilization. The emulsion stability during digestion will determine the available surface area for lipase adsorption in the small intestinal phase and the subsequent lipolysis kinetics (Verkempinck et al., 2018b). However, little is known about the specific influence of the presence of pectin in o/w emulsions on the kinetics of lipid digestion and carotenoid bioaccessibility. In this sense, pectin can be added in emulsions, being present at the oil-water interface or pectin can be located in the aqueous phase of these o/w emulsions. In addition, the structural characteristics of these pectin structures might play an important role during digestion. For example, the methylesterification degree of pectin influences its charge density (Celus et al., 2018) and interactions with different components during digestion (such as calcium, lipase, bile salts and lipophilic components) (Tsujita et al., 2007; McClements, Decker, & Park, 2008; Verrijssen et al., 2014; Espinal-Ruiz et al., 2014b). Therefore, the presented work, explored the effect of the presence of citrus pectin with different methylesterification degree in an emulsified system on the lipid digestion, using the kinetic digestion approach presented by Verkempinck et al. (2018a). Moreover, not only the effect of

145 citrus pectin as mono-emulsifier was evaluated, but also the combination of citrus pectin and a
146 conventional emulsifier stabilizing o/w emulsions was studied. Consequently, the link
147 between lipid digestion and carotenoid bioaccessibility can be quantitatively proven. This
148 allows to evaluate the proposed hypothesis throughout the whole digestion process based on
149 the resulting kinetic parameters. So far in this research field, lipid digestion is mostly studied
150 by evaluation of FFA release in the small intestinal phase. By contrast, this study aimed to
151 quantify multiple lipid digestion species, namely TAG, DAG, MAG and FFA, both in the
152 digest as well as in the micellar fraction. The obtained results can eventually contribute to the
153 development of predictive mathematical (*in silico*) models needed for simulation of lipid
154 digestion of particular food products and to create products for specific consumer groups.

2 Material and methods

Carotenoid enriched oil-in-water (o/w) emulsions were formulated with different emulsifiers (Tween 80, phosphatidylcholine or citrus pectin) or combinations of emulsifiers (section 2.4). Emulsions stabilized with one emulsifier type will be called 'mono-emulsifier emulsions', while emulsions stabilized with pectin and another emulsifier will be called 'di-emulsifier emulsions'. More specifically, the effect of pectin present at the oil-water interface or in the aqueous phase of o/w emulsions on the kinetics of lipid digestion and carotenoid bioaccessibility was studied. Therefore, all emulsions were *in vitro* digested by simulating a gastric and small intestinal phase (section 2.5). The latter was performed using a kinetic approach to evaluate the time dependency of the lipolysis reaction and micellarization of multiple lipolysis products and carotenoids. Digested emulsions will be further referred to as 'digest'. All digests were ultracentrifuged to harvest the aqueous, 'micellar fraction' containing the bioaccessible lipid species and carotenoids. Initial emulsions, digests and micellar fractions were characterized in terms of lipid and carotenoid content (section 2.7 and 2.8). Additionally, the particle charge and size of the initial emulsion, after the gastric phase (chyme) and after 2 hours of small intestinal phase (digestion end point) were determined to evaluate the behavior of the oil droplets during gastrointestinal conditions (section 2.6).

2.1 Materials

Orange carrots (*Daucus carota* cv. Nerac) were bought in a local shop and stored at 4 °C until use. Olive oil was purchased in a local shop. Citrus pectin (CP), Tween 80 (TW) and phosphatidylcholine (PC) were obtained from Sigma Aldrich (Diegem, Belgium). All used chemicals and reagents were of analytical or HPLC-grade and were purchased from Sigma Aldrich (Diegem, Belgium) except for KCl, $MgCl_2(H_2O)_6$, NaOH, heptane, methanol, methyl-tert-butyl-ether and ethyl acetate (Acros Organics, Geel, Belgium); KH_2PO_4; $NaHCO_3$, NaCl,

179 H_2SO_4, ethanol, acetone and trimethylamine (Fisher Scientific, Merelbeke, Belgium); HCl,
180 diethylether and iso-propanol (VWR, Leuven, Belgium); acetone (Carlo Erba, Val-de-Reuil,
181 France); $CaCl_2(H_2O)_2$ (Chem-Lab, Zedelgem, Belgium) and lipid standards (Larodan, Solna,
182 Sweden). Sample preparations were performed with reagent water (organic free, 18.2 MΩ cm
183 resistance), supplied by a Simplicity™ 150 water purification system (Millipore, Billerica,
184 USA).

185 ## 2.2 Pectin preparation

186 High methylesterified CP (HMP) was enzymatically demethylesterified according to the
187 procedure described by Ngouémazong et al. (2011). It was opted use citrus pectin as study
188 vehicle since it is commercially available and has a linear structure, facilitating the
189 interpretation of the obtained data and attributing that to differences in degree of
190 methylesterification only.

191 Briefly, 0.8% (w/v) HMP was incubated with purified extract of carrot pectin methylesterase
192 (PME) at 30 °C for different time periods, resulting in CP with a medium and low degree of
193 methylesterification (DM) (MMP and LMP, respectively). A thermal treatment was used to
194 inactivate PME (4 min, 85 °C) and was followed by a 48-hour dialysis to remove present ions
195 (Spectra/Por®, Molecular weight cut-off = 12-14 kDa). In a final step, pectin samples were
196 lyophilized (Christ Alpha 2-4 LSC, Germany) and stored in a desiccator at room temperature
197 until use. Fourier transform infra-red spectroscopy (IRAffinity-1, Shimadzu, Japan) was used
198 to determine the pectin DM, according to the method described by Kyomugasho et al. (2015).
199 The resulting values for the DM of HMP, MMP and LMP were 82.2 % (± 1.2), 38.3 % (± 0.9)
200 and 10.4 % (± 1.0), respectively and these pectin structures will be further indicated as CP82,
201 CP38 and CP10. In addition, the molecular weight was determined, following the procedure
202 of Shpigelman et al. (2014) with High Performance Size Exclusion Chromatography. For

CP82, CP38 and CP10, a molecular weight was obtained of 58.7 kDa (± 1.3), 54.5 kDa (± 2.0) and 54.1 kDa (± 1.2), respectively, showing that the enzymatic demethylesterification reaction had no significant impact on the molecular weight of the pectin structures. The concentration distribution as function of elution time and the average molecular weights of the different pectin samples is shown in **Figure A in supplementary material**.

2.3 Preparation of carrot-enriched olive oil

Olive oil was enriched with carotenoids from carrot puree according to the method described by Mutsokoti et al. (2015). Carrots were peeled, cut into small pieces (1 x 1 cm) and mixed with demineralized water (1:1) for 1 minute with a kitchen blender (Warington Commercial, Torrington, CT, USA). Carotenoids were released by disrupting their cellular entrapment through a high pressure homogenization step at 100 MPa (Pony NS2006L, Gea Niro Soavi, Düsseldorf, Germany). Olive oil was added (1:5 w/w) and subsequently a blending (1 minute) and a homogenization step (100 MPa, 1 cycle) were performed to allow carotenoid migration from the natural plant matrix into the oil phase. After centrifugation (Optima XPN-80 Ultracentrifuge, Beckman Coulter, Fullerton, CA, USA) with a speed of 165000 g at 4 °C, the carotenoid-enriched olive oil was collected and stored at -80 °C, protected from light and oxygen. The concentration of α- and β-carotene in the obtained enriched oil were 86.3 ± 6.7 and 209.2 ± 16.1 µg per g of enriched oil, respectively. It was explicitly chosen to incorporate carotenoids from a food matrix into the olive oil, rather than using pure carotenoids since in this way a real food system could be approached whereby carotenoids might already be transferred to the oil phase during food preparation prior to digestion.

2.4 Oil-in-water emulsion preparation

First, coarse o/w emulsions were prepared by mixing 5% carrot-enriched oil (w/v) for 10 minutes at 9500 rpm (Ultra-Turrax T25, IKA, Staufen, Germany) to an emulsifier-containing

aqueous phase. The aqueous phase consisted of a mono-emulsifier solution of 0.5% w/v Tween 80 (TW), 1% w/v CP or 1% w/v PC or a di-emulsifier solution of 1% w/v CP mixed with 0.5% w/v TW or 1% w/v PC. A minimum emulsifier amount was used to create stable emulsions. The coarse emulsion was kinetically stabilized with high pressure homogenization at 100 MPa for 1 cycle (Pressure Cell Homogenizer, Stansted Fluid Power LTD., UK). Hereafter, the acidity of all emulsions was adjusted to pH 3 as a preliminar study showed that the emulsions were more stable at low pH (data not shown). All emulsions were stored at 4 °C, protected from light and oxygen for maximally 5 days, being the period in which the emulsions were stable in terms of particle size (data not shown). 'TWCP82' is the abbreviation used to refer to an emulsion stabilized with 0.5% Tween 80 and 1% citrus pectin with a DM of 82. In total, 11 different emulsions were prepared and studied, being referred to as TW; CP82; CP38; CP10; TWCP82; TWCP38; TWCP10; PC; PCCP82; PCCP38 and PCCP10. TW; CP82; CP38; CP10; PC are the 'mono-emulsifier emulsions', while the TWCP82; TWCP38; TWCP10; PCCP82; PCCP38 and PCCP10 emulsions will be referred to as 'di-emulsifier emulsions'.

2.5 *In vitro* digestion

A static *in vitro* digestion procedure was used to investigate the isolated effect of time on lipolysis, micelle formation and carotenoid bioaccessibility. Therefore, the consensus method described by Minekus et al. (2014) as adjusted by Verkempinck et al. (2018a) was applied. Briefly, the gastric phase was simulated by mixing 5 mL of o/w emulsion and 5 mL of reagent water in dark falcon tubes. Subsequently, 7.5 mL simulated gastric fluid, 5 µL calciumchloride (0.3M); 1.6 mL pepsin solution (2000 U/mL in final chyme); 889 µL reagent water and 6 µL HCl (2M) (to adjust the pH to 3) were added. The tubes headspace was flushed with nitrogen, whereafter the chyme was rotated end-over-end (40 rpm) for 2 hours at 37 °C. Hereafter, the small intestinal phase was mimicked by adding 11 mL simulated

intestinal fluid, 40 µl calciumchloride (0.3M); 1.46 mL demineralized water; 2.5 mL of bile solution (10 mM in final digest) and 5 mL of pancreatic solution to 10 mL of chyme. All intestinal fluids were tempered at 37 °C to avoid temperature differences in the digest. The pancreatic solution contained both pancreatin (100 U/mL based on trypsin activity in final digest) and porcine pancreas lipase (to obtain 200 U/mL in the final digest). Furthermore, carotenoid isomerization and degradation during the gastrointestinal conditions was minimized by addition of pyrogallol (0.6% w/v) and α-tocopherol (1.4% w/v) (Lemmens et al., 2011). Nitrogen gas was used to flush the headspaces of the tubes and these tubes were subsequently rotated end-over-end (40 rpm) at 37 °C. The digestion of each emulsion was characterized for seven consecutive time moments (0-120 minutes) to study the time effect on the lipolysis reaction and the micellarization of multiple lipid digestion products and carotenoids. For each time moment, an individual digestion tube was used, resulting in seven independent replications of the simulated digestion process. To inactivate lipase at a particular digestion time in the *in vitro* small intestinal phase, the digest was subjected to a thermal treatment (10 min, 85 °C) and hereafter immediately cooled to 4 °C. The micellar fraction was separated from other components (e.g. enzyme residues and undigested oil) after ultracentrifugation at 165000 g for 68 minutes at 4 °C (Optima XPN-80 Ultracentrifuge, Beckman Coulter, Fullerton, CA, USA). The aqueous, micellar phase was collected, filtered (Chromafil PET filter, 0.2 µm pore size, 25 mm diameter) and analyzed in terms of lipid composition and carotenoid content.

The lipase activity used in the present study was reduced in comparison to the amount suggested by the consensus method of Minekus et al. (2014) (2000 U/mL), but was comparable with the amount used in other, recent digestion studies (63-550 U/mL) (Sarkar et al., 2016; O'Sullivan et al., 2017; Lin & Wright, 2017). However, as explained in a previous study of Verkempinck et al. (2018b), all (emulsified) oil droplets were covered with lipase as

the added amount per digestion tube was still in excess. It must be noted that the obtained results might not be considered for *in vivo* human digestion predictions directly, but do gain more mechanistic insight into the lipolysis reactions.

2.6 Physicochemical properties during digestion

2.6.1 Particle electrical charge

The oil droplets ζ-potential was measured using a dynamic light scattering electrophoresis equipment (Zetasizer NanoZS, Malvern Instruments, Worcestershire, UK). Emulsion, chyme or digest at the digestion end point was diluted 1:100 prior to analysis with reagent water (pH 3), SGF or SIF, respectively. Subsequently, the sample was transferred into a capillary cell equipped with two electrodes to measure the ζ-potential of the studied oil droplets.

2.6.2 Particle size distribution and microstructure

Particles size distributions were measured of all initial emulsions, after 2 hours of gastric phase and after 2 hours of intestinal phase, using a laser diffraction equipment (Beckman Coulter Inc., LS 13 320, Miami, Florida, USA) as mentioned in previous work (Verkempinck et al., 2018b). The reported particle sizes are volume-weighted median sizes (D[v;0.5] value), defined as the particle diameter at which 50% of the particles are smaller than this size. Volume-weighted particle sizes are a more sensitive indicator for instability of emulsions in comparison with surface-weighted particle sizes, as the former largely increases with the presence of a limited number of large particles. In this way, the volume-weighted particle size can be an indicator for possible destabilization phenomena occurring along the digestive tract.

Complementary, microstructures after the gastric phase and at the digestion end point were visualized by differential interference contrast microscopy (Olympus BX41, Olympus Corporation, Tokyo, Japan) equipped with a digital camera (Olympus BX51, Olympus Optical Co. LTD., Tokyo, Japan).

2.7 Quantitative analysis of multiple lipid digestion products

Lipid extraction and analysis was exactly executed as described by Verkempinck et al. (2018b). The approach described by Verkempinck et al. (2018b) was used for analysis of the obtained lipid data. Stoichiometric reactions and mass balances were used to calculate the percentage of digested TAG at each time moment in the small intestine (%) and will be referred to as 'lipolysis extent'. This was based on the difference between the TAG amount in the emulsion (analytical value) and the sum of multiple lipolysis products released in the small intestine (MAG+FFA+GLY-H_2O). MAG and FFA (analytical values) will be expressed in concentrations ($mg/g_{emulsion}$). It must be noted that DAG were detected, but below the quantification limit and were therefore not taken into account in the data analysis.

2.8 Carotenoid analysis

Carotenoids were extracted and quantified by exactly performing the procedure described before by Verkempinck et al. (2018a). Carotenoid identification and quantification was done at the wavelength of maximal absorption for α- and β-carotene (450 nm). *In vitro* carotenoid bioaccessibility (BAC) is expressed as a percentage value and is defined as the ratio of carotenoid amount incorporated into the micelle fraction to the initial carotenoid amount present in the emulsion, both expressed per g initial emulsion.

2.9 Statistical analysis

The statistical software programs JMP (JMP Pro13, SAS Institute Inc., Cary, NC, USA) and SAS (version 9.4, SAS Institute Inc., Cary, NC, USA) were used to perform all statistical analysis. Significant differences in particles electrical charge and sizes were conducted by one way ANOVA and the Tukey's Studentized Range Post-hoc test with a 95% level of significance ($P<0.05$). All particle charge and size measurements were performed in duplicate.

Nonlinear regression was used to model the experimental data obtained through the kinetic study for lipid digestion and carotenoid bioaccessibility. The empirical, most simple model best describing the experimental data was selected using model discrimination. As described before by Verkempinck et al. (2018b), a fractional conversion model was chosen and is characterized by a first order reaction until attainment of a plateau value (equation 1). Hereby C (%) is the studied parameter at time t in the simulated intestinal phase; C_f (%) is the final, maximum of the studied parameter that can be obtained with the imposed conditions; C_0 (%) is the initial studied parameter at time 0 in the simulated intestinal phase; k (min^{-1}) is the reaction rate constant of the studied process and t (min) is time in the simulated intestinal phase. The TAG concentration at the start of the simulated intestinal phase was assumed to be equal to the TAG concentration present in the initial emulsion.

$$C = C_f + (C_0 - C_f) \cdot e^{(-kt)} \qquad \text{(equation 1)}$$

This fractional conversion model could be simplified as lipid digestion at the start of the simulated intestinal phase could be neglected (equation 2). Therefore, the concentrations of MAG; FFA and GLY, and carotenoid concentration in the micellar fraction were assumed to be zero (C_0=0) at this initial stage of digestion.

$$C = C_f \cdot (1 - e^{(-kt)}) \qquad \text{(equation 2)}$$

The jointly estimated parameters (C_f and k) were determined and visualized by calculating the 90% joint confidence regions (JCRs). If regions of different samples overlap, it could be stated that the overall kinetics of these samples are not significantly different.

3 Results and discussion

Different carrot-enriched o/w emulsions were submitted to an *in vitro* digestion procedure, consisting on a simulated gastric and small intestinal phase. The emulsions were stabilized with different *(i)* mono-emulsifier types (Tween 80 (TW); phosphatidylcholine (PC) or citrus pectin (CP)) or *(ii)* di-emulsifier solutions (TWCP or PCCP) to evaluate the role of the pectin fiber in both the lipolysis as well as the carotenoid bioaccessibility reaction. The intestinal phase was studied in a kinetic way in order to gain more mechanistic insight in the process of lipolysis and micellarization of multiple lipid digestion products and carotenoids (sections 3.2 and 3.3). Particles electrical charge and size were determined during digestion as the different emulsifier types and combinations might have a specific influence on the emulsion behavior under simulated gastrointestinal conditions (sections 3.1.1 and 3.1.2, respectively).

3.1 Evolution of physicochemical changes during *in vitro* digestion

3.1.1 Particle electrical charge

The particle electrical charge was measured for the emulsion, after the gastric phase and at the small intestinal digestion end point. This can provide more information about the organization of the emulsifier(s) at the oil-water interface and the phenomena that occur during simulated gastrointestinal conditions. The obtained particle charges are shown in **Table 1**.

The ζ-potential of all initial emulsions with a pH of 3 varied between 3 and -31 mV depending on the emulsifier type and combination used (**Table 1**). The emulsion stabilized with the non-ionic TW had an initial ζ-potential of -7.84 ± 1.19 mV. These negative charges might be attributed to the presence of impurities in the oil phase (e.g. free fatty acids; FFA) or the preferential adsorption of hydroxyl ions from the continuous phase to the hydrophilic head of the surfactant (McClements, 2016). By contrast, the PC emulsion was slightly positively charged (2.43 ± 0.24 mV), which could be explained by the shielding of the negatively

charged phosphate groups by hydrogen ions at low pH (Lin et al., 2014). The ζ-potential of the CP emulsions was significantly influenced by the pectin DM and was more negative for CP10 compared to CP38 and CP82. This was attributed to the presence of more negatively chargeable carboxylic groups in LMP compared to MMP and HMP, even at low pH. By contrast, the TWCP emulsions had similar charges as the TW emulsion (**Table 1**) and no effect of DM was observed. Therefore, it could be hypothesized that the small molecule surfactant TW (± 1200-1350 Da) adsorbed much faster at the oil-water interface than the large pectin structures (± 55000 Da). Consequently, the latter remained in the aqueous phase and did not attribute to the particle electrical charge. Oppositely, the charge of the PCCP emulsions showed an effect of pectin DM, being more negative when LMP was used for emulsion stabilization in comparison with MMP or HMP. In the case of these PCCP emulsions, probably both PC and CP adsorbed at the interface. More specifically, it can be postulated that a multilayer emulsion was formed with first phosphatidylcholine surrounding the oil droplet, followed by the oppositely charged pectin structures. As suggested by Guo et al. (2017), this multilayer emulsion might be more resistant to lipolysis than the monolayer emulsions.

After simulation of the gastric phase, an increase in particle charge was measured (**Table 1**). This was attributed to the interactions between the negatively charged oil-water surfaces and the added ions (such as Ca^{2+}, K^{+} and H^{+}). In general, similar trends were observed as in the initial emulsions. In this sense, the TW and TWCP emulsions had similar particle charges initially as well as after the gastric phase. The emulsions having CP at the interface (i.e. CP and PCCP emulsions) still showed a more negative charge with lower pectin DM (charge HMP > MMP > LMP).

More negatively charged particles were observed in all cases at the end of the intestinal phase (**Table 1**). Among all added fluids used to simulate the small intestinal phase, lipase was

394 responsible for hydrolysis of triacylglycerol (TAG) into diacylglycerol (DAG),
395 monoacylglycerol (MAG), FFA and glycerol (GLY). According to Singh, Ye & Horne
396 (2009), the more negative charge could be ascribed to the presence of structures formed
397 containing bile salts and phospholipids, and as well to FFA release which are negatively
398 charged at pH 7. An effect of pectin DM was no longer observed in the pectin-containing
399 samples.

400 ***3.1.2 Particle size distribution and microstructure***

401 The particle size distribution and microstructure were studied before as well as during
402 digestion to evaluate the stability of the oil droplets along the simulated digestive tract. The
403 particle size distributions are shown in **Figure 1**, while all microstructures are depicted in
404 **Figure B** (supplementary material).

405 All initial emulsions had a particle size in the sub-micron range, with median oil droplet sizes
406 between 1.01 and 1.82 µm (**Table A, supplementary material**). The TW emulsion had the
407 smallest median droplet size (1.27 ± 0.10 µm) of all mono-emulsifier emulsions (i.e.
408 emulsions stabilized with one emulsifier type) and the PC emulsion had the largest droplet
409 size (1.82 ± 0.07 µm). This might indicate that PC is not that efficient in stabilizing o/w
410 emulsions compared to TW. McClements & Gumus (2016) described that PC is mostly used
411 in combination with other emulsifiers, as PC has only an intermediate hydrophobicity. In case
412 of the CP emulsions, the CP38 emulsion had significant smaller oil droplets than the CP82
413 and CP10 emulsions. Similar results were observed by Verrijssen et al. (2015), whereby
414 MMP exhibited smaller oil droplets. This observation was explained by the block-wise
415 organization of the present hydrophilic and hydrophobic galacturonic acid molecules in
416 MMP. TWCP emulsions had smaller particle sizes compared to both the TW and CP
417 emulsion. As was mentioned in section 3.1.1, it was hypothesized that for the TWCP
418 combination, the small molecule TW covered the complete interface, while pectin remained

in the aqueous phase. However, the presence of pectin might have created a competitional effect for the interface, whereby TW moved slightly faster to the interface and eventually led to smaller particle sizes for the TWCP emulsions. A similar trend of smaller particle sizes was observed in the di-emulsifier emulsion PCCP, in comparison with their mono-emulsifier emulsions. Additionally, an effect of pectin DM was observed in pectin-containing emulsions. More specifically, slightly smaller oil droplets were created using MMP as emulsifier compared to LMP or HMP. It is known that the initial oil droplet size of emulsions is an important characteristic which can have a big impact upon lipolysis kinetics (Zhang et al., 2016; Salvia-Trujillo et al., 2017). Nevertheless, the differences in initial oil droplet in the presented study are rather small and the emulsifier structure and organization at the interface might play a more dominating and so crucial role on the emulsions behavior during digestion and subsequently lipolysis kinetics.

Simulation of the gastric conditions influenced the particle size of the studied emulsions (**Figure 1 and Table A in supplementary material**). Two different situations were observed. On the one hand, the particle size distributions of the TW and PCCP emulsions remained similar, while on the other hand bimodal particle size distributions were observed for the TWCP, PC and CP emulsions (**Figure 1**). TW is known to be an acid stable emulsifier (Marciani et al., 2006; Verkempinck et al., 2018b). However TWCP emulsions were unstable in the gastric phase, which could be due to the presence of pectin in the aqueous phase, inducing coalescence and flocculation phenomena. The PCCP combination resulted in acid stable emulsions, which could be explained by the multilayer organization at the oil-water interface, being more resistant to the gastric conditions. By contrast, the emulsions stabilized with PC or CP only were acid unstable. This could be attributed to the addition of ions (such as Ca^{2+}, K^{+} and H^{+}) and consequently shift to more neutral particle charge (**Table 1**) which could have compromised the emulsion stability. In case of the acid unstable emulsifier

(combination), coalescence phenomena caused the observed particle size increase and were also visualized by microscopic pictures (**Figure B, supplementary material**).

Multimodal particle size distributions were detected at the digestion end point (**Figure 1**). The first intensity peak (1-3 µm) might be related to the formed micellar fraction and other vesicles, containing bioaccessible lipolysis products and carotenoids. The second main intensity peak (10-30 µm) might be related to the presence of undigested oil. For the TW emulsion, the first intensity peak is more pronounced than the second, which might be related to a relatively high lipolysis extent. In all other cases, the intensity peak related to undigested oil, was equally or more intense than the first peak. In fact, the presence of undigested oil at the digestion end point was also confirmed by microscopic pictures (**Figure B, supplementary material**). These observations showed that on the one hand the lipolysis reaction was incomplete for all the emulsions studied, but that on the other hand structures with sizes of 1-3 µm were present which can contain bioaccessible lipolysis products and carotenoids.

In conclusion, the emulsions can be divided into two categories: acid stable emulsifier(s) (combinations) (i.e. TW and PCCP) and acid unstable emulsifier(s) (combinations) (i.e. TWCP, PC and CP). The increased particle size in the latter case compared to the initial emulsion, might have a direct impact upon lipolysis kinetics as the particle size at the end of the gastric phase determines the available area for digestive enzymes to adsorb in the intestinal phase. At the end of the small intestinal phase, multimodal particle size distributions were observed for all emulsions. The two main intensity peaks can be associated with *(i)* (colloidal) structures which can contain multiple lipid digestion products and carotenoids or *(ii)* large, undigested oil droplets.

3.2 Study of lipid digestion kinetics as influenced by the presence of citrus pectin

Emulsion lipid digestion mainly occurs in the small intestine, where lipase hydrolyses TAG into DAG, MAG, FFA and GLY. Simultaneously, bile salts remove the formed multiple lipolysis products from the oil interface to build mixed micelles. In the present study, small intestinal lipid digestion of several emulsions was executed in a kinetic way. In this sense, the effect of time on TAG hydrolysis and formation of multiple lipid digestion products in the small intestinal phase can be studied. The obtained experimental data were modelled using nonlinear regression. A fractional conversion model (equation 2) best described the data. It is characterized by a linear increase (k-value) until attainment of a final plateau value (C_f). Consequently, differences among the studied emulsions could be quantitatively evaluated. In a next step, the jointly estimated parameters (k and C_f) were used as input for joint confidence region (JCR) (90%) analysis to determine whether these parameters were significantly different among all emulsions studied. The kinetic digestion approach and corresponding data analysis already showed large potential in clarifying differences in lipolysis kinetics and micelle formation in previous studies performed at our research unit (Salvia-Trujillo et al., 2017; Verkempinck et al., 2018b). The obtained kinetic data for the small intestinal lipolysis and the mixed micelle formation kinetics will be discussed in sections 3.2.1 and 3.2.2, respectively.

3.2.1 Lipid digestion kinetics in the small intestinal phase

In all cases, a steady-state condition was reached within the 2 hours of simulated small intestinal digestion (**Figure 2**). However, depending on the emulsifier type and combination used for emulsion stabilization, major differences were observed regarding *(i)* the rate with which the steady-state condition was reached and *(ii)* the final concentration of the different lipid species (**Table 2**).

Evaluating the *k*-values of the TAG hydrolysis reaction of the pectin-based emulsions (i.e. all emulsions containing pectin) revealed that the pectin DM had a major effect on the reaction rate constants (**Table 2**). CP10-based emulsions (i.e. CP10; TWCP10 and PCCP10 emulsions) reached the steady-state conditions much faster than CP38- or CP82-based emulsions. This suggests that the interface of CP10-based emulsions is of good quality for lipase adsorption and led to a fast lipolysis reaction. This can be attributed to a less compact organization of CP10 at the oil-water interface due to more present charged carboxylic groups, thus creating more inter-molecular repulsive forces and probably leave accessible spaces at the interface. Consequently, the interface can be more easily reached by digestive components. However, LMP is known to interact in a high extent with calcium ions (Espinal-Ruiz et al., 2014a). These ions are needed to remove the lipid digestion products from the oil surface. Consequently, it can be hypothesized that in the case of CP10-based emulsions, the lipolysis reaction reached its steady-state condition fast due to a relatively accessible oil-water interface which is thereafter quickly covered by lipolysis products since these were no longer removed by the calcium ions due to pectin-calcium interactions. When combining TW with CP to stabilize an emulsion, an increased *k*-value of the lipolysis reaction was observed (ranging from 0.092 to 0.253 min^{-1}) in comparison with the TW emulsion (0.086 min^{-1}). An opposite trend was observed when comparing the *k*-values of the PC versus PCCP emulsions as in the case of the PC emulsion, the *k*-value was 0.233 min^{-1}, while it was ranging from 0.052 to 0.147 min^{-1} for the PCCP di-emulsifier emulsions. For the PCCP emulsion it was assumed that both emulsifier types were adsorbed at the oil-water interface. The presence of pectin at the interface might have led to interactions between pectin and the digestive components, slowing down the TAG hydrolysis. In addition, presence of the large pectin structures at the interface might hinder or retard the adsorption of lipase, bile and calcium at the oil droplet surface.

By contrast, the final percentage of digested TAG was mainly determined by the emulsifier (combination) used for emulsion stabilization (**Table 2**). TW emulsions presented the highest amount of digested TAG (83%), followed by the TWCP (72-77%), PCCP (6.5-7.3%), CP (4.9-5.5%) and PC (4.6%) emulsions. In case of the TWCP di-emulsion, the addition of pectin to the emulsion lowered the lipolysis extent in comparison with the TW mono-emulsion. The data of the particle charge (section 3.1.1) suggested that in case of these TWCP di-emulsions, TW was adsorbed at the oil-water interface, while the CP structures were located in the continuous phase. Consequently, it can be postulated that the CP structures present in the aqueous phase interact with components within the intestinal juices, such as lipase and bile salts, inhibiting the lipid digestion extent. A study of Espinal-Ruiz et al. (2014a) evaluated the interactions between pectin and individual components present during digestion and showed that pectin interacts with bile, lipase and calcium. When comparing the lipolysis extent of the PC, CP and PCCP emulsions a different trend could be observed. Namely, the combination of PC and CP at the interface improved the lipolysis extent in comparison with the mono-emulsifier emulsions. This could be attributed to presence of a double layer in the PCCP emulsions, improving the gastric stability. The PC and CP emulsions, unlike the PCCP emulsions, were unstable under gastric conditions (section 3.1.2). Consequently, coalescence phenomena occurred, resulting in oil droplets with a lower active surface area at the beginning of the small intestinal phase in case of the PC and CP emulsions.

Significant differences in the correlated parameters among all emulsions were visualized by JCR analysis, depicted in **Figure C in supplementary material**. These results confirm the observations described above: the *k*-values of the TAG hydrolysis reaction are predominantly determined by the DM of the present CP structures, while the final digested TAG percentages were mainly affected by the emulsifier (combination) used for emulsion formulation.

It could also be observed that the TAG hydrolysis was incomplete in all cases (**Table 2**). In case of the acid unstable emulsions (section 3.1.2), this could be partially attributed to the increased particle size at the end of the gastric phase. Consequently, a lower active surface area is available for lipase to adsorb. Similar observations were conducted in a study of Salvia-Trujillo (2017), showing that emulsions with large emulsified oil droplet sizes (≈ 15 µm) were digested in a lower extent compared to emulsions with small emulsified oil droplet sizes (≈ 2 µm). The lipolysis reaction was also incomplete for acid stable emulsions. It can be hypothesized that in the case where pectin is adsorbed at the oil-water interface (i.e. CP and PCCP emulsions), pectin can inhibit the adsorption of digestive components (such as lipase, bile and calcium). As a result, these digestive components can no longer fulfill their function, leading to a diminished TAG hydrolysis reaction. Moreover, in the case of the PCCP emulsions, it was postulated that a multilayer emulsions was formed, which is assumed to be more resistant to lipase hydrolysis (section 3.1.1) (Guo et al., 2017). From **Table 2**, it can also be observed that emulsions containing CP82 led to a lower lipolysis extent in comparison to emulsions composed with CP10. The more hydrophobic HMP is known to interact in a higher extent with lipase, bile and phospholipids, in comparison with the more hydrophilic MMP and LMP (Tsujita et al., 2007; Espinal-Ruiz et al., 2014b) which might have diminished the lipolysis extent of the CP82-based emulsions.

In addition, it could be noted that the emulsions where pectin is located at the interface, present a relatively low TAG hydrolysis extent. Consequently, it can be stated that the presence of pectin at the oil-water interface has a negative effect on the TAG hydrolysis extent. By contrast, the emulsions stabilized by TW showed a more complete lipolysis reaction so the presence of pectin structures in the continuous aqueous phase does not significantly change the lipolysis reaction extent (**Figure C1, supplementary material**).

By digesting TAG molecules, a simultaneous release of MAG and FFA in the digest was detected (**Figure 2**). It must be noted that DAG were detected but below the quantification limit so were not taken into account in the discussion. GLY concentrations present in the digest were relatively low and no time effect could be observed, so these observations were omitted from the data analysis. Regarding the kinetics of MAG and FFA, similar observations were conducted as in the TAG hydrolysis reaction. In this sense, the release rate constant was mainly influenced by the pectin DM, while the extent of release MAG and FFA was determined by the emulsifier(s) used for emulsion stabilization (**Figure 2, Table 2 and Figure C2 and C3 in supplementary material**). Additionally, for all pectin containing emulsions, higher *k*-values were observed for MAG release in comparison to FFA release. In other words, the steady-state condition was reached slower for FFA release. This might be attributed to a further conversion of MAG into FFA and GLY (Mu & Høy, 2004; Tokle, Mao, & McClements, 2013).

In conclusion, it can be stated that the correlated parameters *k* and C_f can be influenced by different emulsion characteristics. More specifically, *k*-values were mainly influenced by the pectin DM, while the extent of TAG hydrolysis and subsequent FFA and MAG release was determined by the emulsifier type and combination present in the emulsion. These results also showed that specific emulsion characteristics might be selected with the aim of tailoring lipid digestion kinetics.

3.2.2 Composition and formation kinetics of the micellar fraction

The hydrolysis of TAG molecules led to the release of MAG and FFA in the digest and a simultaneous micellarization of these lipid digestion products could be observed. This is in line with the mechanism of lipid digestion and micelle formation described in literature (Mun, Decker, & McClements, 2007; Singh, Ye, & Horne, 2009). The micellarization kinetics were

589 strongly related to the kinetics of FFA and MAG release in the digest (section 3.2.1) and are
590 summarized below.

591 Similarly to the observations in the digest, the reaction rate constant *k* for MAG and FFA
592 micellarization was mainly effected by the pectin DM (**Table 2**). In most cases, the *k*-values
593 for TAG hydrolysis, MAG and FFA release in the digest were of the same magnitude for a
594 certain emulsion type, showing that the lipolysis reaction and ensuing release of MAG and
595 FFA are not the rate limiting steps in the lipid digestion process. The final concentration lipid
596 digestion products present in the micellar fraction was predominantly determined by the
597 emulsifier (combination) used for emulsion stabilization as was also observed for the lipolysis
598 reaction. It can be stated that the presence of pectin in emulsions does not have an
599 unambiguous effect on the lipolysis and subsequent micelle formation kinetics. On the one
600 hand, pectin can interact with lipolysis components (such as lipase, bile salts and calcium),
601 diminishing the final lipolysis extent. On the other hand, the presence of pectin can improve
602 the quality of the oil-water interface or improve the emulsion stability during gastrointestinal
603 simulation, leading to an increased lipid digestion extent and subsequent release and
604 micellarization of MAG and FFA.

605 The obtained data were also evaluated by JCR (90%) analysis and the results are depicted in
606 **Figure C (supplementary material)**. These graphs confirm the above described trends and
607 clearly show that the TW and TWCP emulsions present higher MAG and FFA concentrations
608 in the micellar fraction than the PC, CP and PCCP emulsions. Moreover, it can be observed
609 that not all MAG and FFA were micellarized which could be attributed to interactions
610 between the lipid digestion products and pectin, calcium and other salts present in the
611 simulated intestinal fluid.

612 In conclusion, the emulsifier (combination) used for emulsion stabilization had a significant
613 effect on the final micellarised concentrations of MAG and FFA. By contrast, the reaction rate

614 constant of the incorporation of MAG and FFA into mixed micelles was mainly determined
615 by the pectin DM. These differences in composition of these mixed micelles will most likely
616 have an important effect on the carotenoid bioaccessibility kinetics, which will be further
617 discussed in section 3.3.1.

618 3.3 Study of carotenoid bioaccessibility kinetics as influenced by the
619 presence of citrus pectin

620 Carotenoid bioaccessibility (BAC) was studied to evaluate *(i)* the time dependency of
621 carotenoid micellarization and *(ii)* its relationship with lipolysis kinetics. Therefore,
622 carotenoid BAC kinetics were determined in parallel with the lipolysis kinetics, so using the
623 same kinetic approach as described in section 3.2. Briefly, the small intestinal phase was
624 simulated in a kinetic way, whereafter the experimental data were modelled with a fractional
625 conversion model. This resulted in the obtainment of a reaction rate constant k and final BAC_f
626 value of the process. Subsequently, these jointly estimated parameters were used as input to
627 determine 90% JCR. In this way, significant differences among all studied emulsions could be
628 determined and visualized.

629 *3.3.1 Carotenoid bioaccessibility kinetics*

630 Micellarisation of α- and β-carotene increased linearly as function of small intestinal digestion
631 time until a steady-state condition was reached (**Figure 3**). This steady-state condition was
632 reached in all cases within two hours of small intestinal digestion. Similar to lipid digestion
633 and micelle formation, the kinetics of carotenoid bioaccessibility (BAC) were influenced by
634 the emulsifier type, emulsifier combination and pectin DM stabilizing the o/w emulsions
635 (**Figure 3, Table 3 and Figure D in supplementary material**) and will be summarized
636 below.

637 The highest carotenoid micellarization rate constant was observed in case of the PC emulsion
638 (0.283 min^{-1} for α-carotene and 0.134 min^{-1} for β-carotene), while the other emulsions showed
639 similar *k*-values, varying between 0.013 and 0.073 min^{-1}. The carotenoid micellarization rate
640 constant of emulsion having pectin adsorbed at the oil-water interface (i.e. CP and PCCP
641 emulsions) were lower for CP82 than for CP38 and CP10. By contrast, when pectin was
642 present in the aqueous phase (i.e. TWCP emulsions) a reverse trend was observed (CP82 >
643 CP38 > CP10). It can be hypothesized that in the former case, the more hydrophobic CP82
644 interacts in a higher extent with the lipophilic carotenoids compared to CP38 and CP10,
645 retarding the incorporation of carotenoids into the micellar fraction. By contrast in the case
646 where CP is present in the aqueous phase, CP10 might have led to an increased viscosity of
647 the digest by interactions with calcium, which in turn can slow down the migration of
648 carotenoids towards the mixed micelles (Verrijssen et al., 2015).

649 The final carotenoid BAC was predominantly determined by the emulsifier(s) used for
650 emulsions stabilization. In this sense, the TW emulsion presented the highest carotenoid BAC
651 values (69-82%), followed by the TWCP emulsions (37.8-64.3%), the PCCP emulsions (19.4-
652 25.4%) and finally the PC (13.8-17.1%) and CP (11.1-19.4%) emulsions, which presented the
653 lowest BAC_f-values. The addition of pectin in the case of TW emulsions, led to a diminished
654 amount of micellarized carotenoids, namely from 82% to 40-64% for α-carotene and from
655 69% to 38-56% for β-carotene. This can be explained by the interactions occurring between
656 pectin structures and the lipophilic carotenoids. In addition, the presence of pectin at the
657 interface does not improve the carotenoid bioaccessibility. More specifically, the final
658 carotenoid BAC values obtained in case of the CP and PCCP emulsions were rather low and
659 ranged from 11% to 25%. This could be related to the low amount of digested TAG molecules
660 (section 3.2.1). In this way, carotenoids remained entrapped in the undigested oil and could
661 not be transferred to mixed micelles.

3.3.2 Relation between the kinetics of lipid digestion and carotenoid bioaccessibility

The estimated parameters k and C_f of the micellarization of MAG, FFA and β-carotene were used to evaluate the relation between the two micellarization phenomena (**Figure E, supplementary material**) as previous research has indicated that there is a strong link between the lipid digestion reaction and carotenoid bioaccessibility (Salvia-Trujillo et al., 2017; Verkempinck et al., 2018a).

For the *k*-values, it can be seen that no direct link was observed between the rate constants of lipid digestion and carotenoid bioaccessibility. This can be attributed to the presence of pectin with different DM, which effects the reaction differently depending on the emulsion composition. Regarding the final micellarized amounts of MAG, FFA and carotenoids, an strong interrelation could be observed between the MAG and FFA concentrations incorporated into micelles and the extent of carotenoid bioaccessibility. In this sense, a higher concentration of incorporated MAG and FFA into mixed micelles, eventually led to a higher carotenoid bioaccessibility.

In the context of satiety and human health, some emulsion compositions can be of interest. For example, the TW mono-emulsion and TWCP di-emulsion present a relatively slow lipid digestion rate and finally result in a high lipolysis rate and relatively high carotenoid bioaccessibility. A slow lipid digestion increases the hormone-induced satiety and slows down gastric emptying, which consequently reduces energy intake (Ohlsson et al., 2014). Additionally, a high lipolysis extent is desired as undigested lipids in the large intestine are associated with several negative effects, such as a bloated feeling, steatorrhoea and an increased risk of tumor development in the colon (Hoyles & Wallace, 2010).

4 Conclusions

The presented work aimed to explore the effect of the presence of pectin in emulsions on the kinetics of lipid digestion and carotenoid bioaccessibility. The emulsifier(s) (combination) used for emulsion stabilization determined the composition of the oil-water interface and surrounding medium, but however presented similar small initial particle sizes. Subsequently, the different emulsion compositions affected the particle size and charge during digestion and moreover, had a significant impact on the lipid digestion reaction and micellarization of multiple lipolysis products and carotenoids. The reaction rate constant *k* for lipid hydrolysis was mainly influenced by the pectin DM. By contrast, the final percentage digested TAG, released MAG and FFA, and micellarized MAG, FFA and carotenoids was predominantly influenced by the emulsifier(s) (combination) used for emulsion stabilization. An interrelation was observed between the extent of micellarization of MAG, FFA and β-carotene. Namely, a higher concentration of incorporated MAG and FFA into the micellar fraction is associated with a higher final carotenoid bioaccessibility. Finally, it can be stated that the intake of fibers alters lipid digestion extent which was hypothesized before the study. Moreover, the results proved that targeted emulsion design can be used as a tool for tailoring lipid digestion and/or carotenoid bioaccessibility.

Acknowledgment

This research was financially supported by the Institute for the Promotion of Innovation through Science and Technology in Flanders (IWT-Vlaanderen). S.H.E. Verkempinck is a Doctoral Researcher funded by IWT-Vlaanderen (Grant No. 141469). L. Salvia-Trujillo is a Postdoctoral Researcher funded by the European Union's Horizon 2020 research and innovation programme under the Marie Sklodowska-Curie grant agreement No. 654924.

Declaration of interests

The authors of the present work declare no conflict of interests.

References

Borel, P., Grolier, P., Armand, M., Partier, A., Lafont, H., Lairon, D. et al. (1996). Carotenoids in biological emulsions: Solubility, surface-to-core distribution, and release from lipid droplets. *Journal of Lipid Research, 37,* 250-261.

Celus, M., Salvia-Trujillo, L., Kyomugasho, C., Maes, I., Van Loey, A. M., Grauwet, T. et al. (2018). Structurally modified pectin for targeted lipid antioxidant capacity in linseed/sunflower oil-in-water emulsions. *Food Chemistry, 241,* 86-96.

Deming, D. M. & Erdman, J. W. (1999). Mammalian carotenoid absorption and metabolism. *Pure and Applied Chemistry, 71,* 2213-2223.

Espinal-Ruiz, M., Parada-Alfonso, F., Restrepo-Sanchez, L. P., Narvaez-Cuenca, C. E., & McClements, D. J. (2014a). Impact of dietary fibers [methyl cellulose, chitosan, and pectin] on digestion of lipids under simulated gastrointestinal conditions. *Food & Function, 5,* 3083-3095.

Espinal-Ruiz, M., Parada-Alfonso, F., Restrepo-Sánchez, L. P., Narváez-Cuenca, C. E., & McClements, D. J. (2014b). Interaction of a dietary fiber (pectin) with gastrointestinal components (bile salts, calcium, and lipase): A calorimetry, electrophoresis, and turbidity study. *Journal of Agricultural and Food Chemistry, 62,* 12620-12630.

Golding, M. & Wooster, T. J. (2010). The influence of emulsion structure and stability on lipid digestion. *Current Opinion in Colloid & Interface Science, 15,* 90-101.

Guo, Q., Ye, A., Bellissimo, N., Singh, H., & Rousseau, D. (2017). Modulating fat digestion through food structure design. *Progress in Lipid Research, 68,* 109-118.

Hoyles, L. & Wallace, R. J. (2010). Gastrointestinal tract: Fat metabolism in the colon. In *Timmis K.N. (eds) Handbook of hydrocarbon and lipid microbiology* (pp. 3111-3118). Berlin, Heidelberg: Springer.

Hur, S. J., Kim, Y. C., Choi, I., & Lee, S. K. (2013). The effects of biopolymer encapsulation on total lipids and cholesterol in egg yolk during *in vitro* human digestion. *International Journal of Molecular Sciences, 14,* 16333-16347.

Kyomugasho, C., Christiaens, S., Shpigelman, A., Van Loey, A. M., & Hendrickx, M. E. (2015). FT-IR spectroscopy, a reliable method for routine analysis of the degree of methylesterification of pectin in different fruit- and vegetable-based matrices. *Food Chemistry, 176,* 82-90.

Lemmens, L., Colle, I. J. P., Van Buggenhout, S., Van Loey, A. M., & Hendrickx, M. E. (2011). Quantifying the influence of thermal process parameters on *in vitro* β-carotene bioaccessibility: A case study on carrots. *Journal of Agricultural and Food Chemistry, 59,* 3162-3167.

746 Lin, X., Wang, Q., Li, W., & Wright, A. J. (2014). Emulsification of algal oil with soy
747 lecithin improved DHA bioaccessibility but did not change overall *in vitro*
748 digestibility. *Food & Function, 5,* 2913-2921.

749 Lin, X. & Wright, A. J. (2017). Pectin and gastric pH interactively affect DHA-rich emulsion
750 *in vitro* digestion microstructure, digestibility and bioaccessibility. *Food*
751 *Hydrocolloids*.

752 Marciani, L., Wickham, M. S. J., Bush, D., Faulks, R., Wright, J., Fillery-Travis, A. J. et al.
753 (2006). Magnetic resonance imaging of the behaviour of oil-in-water emulsions in the
754 gastric lumen of man. *2007/03/08,* 331-339.

755 McClements, D. J. (2016). *Food emulsions: Principles, practices and techniques*. (Third ed.)
756 Boca Raton, Florida, USA: CRC Press (Taylor & Francis Group).

757 McClements, D. J. & Decker, E. A. (2009). Controlling lipid bioavailability using emulsion-
758 based delivery systems. In D.J.McClements (Ed.), *Designing functional foods* (pp.
759 502-546). New York: CRC Press.

760 McClements, D. J., Decker, E. A., & Park, Y. (2008). Controlling lipid bioavailability through
761 physicochemical and structural approaches. *Critical Reviews in Food Science and*
762 *Nutrition, 49,* 48-67.

763 McClements, D. J. & Gumus, C. E. (2016). Natural emulsifiers – Biosurfactants,
764 phospholipids, biopolymers, and colloidal particles: Molecular and physicochemical
765 basis of functional performance. *Advances in Colloid and Interface Science, 234,* 3-26.

766 Minekus, M., Alminger, M., Alvito, P., Ballance, S., Bohn, T., Bourlieu, C. et al. (2014). A
767 standardised static *in vitro* digestion method suitable for food - an international
768 consensus. *Food & Function, 5,* 1113-1124.

769 Mu, H. & Høy, C. K. (2004). The digestion of dietary triacylglycerols. *Prog in Lipid Res, 43,*
770 105-133.

771 Mun, S., Decker, E. A., & McClements, D. J. (2007). Influence of emulsifier type on *in vitro*
772 digestibility of lipid droplets by pancreatic lipase. *Food Research International, 40,*
773 770-781.

774 Mun, S., Decker, E. A., Park, Y., Weiss, J., & McClements, D. J. (2006). Influence of
775 interfacial composition on *in vitro* digestibility of emulsified lipids: Potential
776 mechanism for chitosan's ability to inhibit fat digestion. *Food Biophysics, 1,* 21-29.

777 Mutsokoti, L., Panozzo, A., Musabe, E. T., Van Loey, A., & Hendrickx, M. (2015).
778 Carotenoid transfer to oil upon high pressure homogenisation of tomato and carrot
779 based matrices. *Journal of Functional Foods, 19, Part A,* 775-785.

780 Ngouémazong, E. D., Tengweh, F. F., Duvetter, T., Fraeye, I., Van Loey, A., Moldenaers, P.
781 et al. (2011). Quantifying structural characteristics of partially de-esterified pectins.
782 *Food Hydrocolloids, 25,* 434-443.

783 O'Sullivan, C., Davidovich-Pinhas, M., Wright, A. J., Barbut, S., & Marangoni, A. G. (2017).
784 Ethylcellulose oleogels for lipophilic bioactive delivery - effect of oleogelation on *in*
785 *vitro* bioaccessibility and stability of beta-carotene. *Food & Function, 8,* 1438-1451.

786 Ohlsson, L., Rosenquist, A., Rehfeld, J. F., & Härröd, M. (2014). Postprandial effects on
787 plasma lipids and satiety hormones from intake of liposomes made from fractionated
788 oat oil: two randomized crossover studies. *Food & Nutrition Research, 58,* 24465.

789 Pasquier, B., Armand, M., Castelain, C., Guillon, F., Borel, P., Lafont, H. et al. (1996).
790 Emulsification and lipolysis of triacylglycerols are altered by viscous soluble dietary
791 fibres in acidic gastric medium in vitro. *Biochemical Journal, 314,* 269-275.

792 Salvia-Trujillo, L., Verkempinck, S. H. E., Sun, L., Van Loey, A. M., Grauwet, T., &
793 Hendrickx, M. E. (2017). Lipid digestion, micelle formation and carotenoid
794 bioaccessibility kinetics: Influence of emulsion droplet size. *Food Chemistry, 229,*
795 653-662.

796 Sarkar, A., Murray, B., Holmes, M., Ettelaie, R., Abdalla, A., & Yang, X. (2016). *In vitro*
797 digestion of pickering emulsions stabilized by soft whey protein microgel particles:
798 Influence of thermal treatment. *Soft Matter, 12,* 3558-3569.

799 Schmidt, U. S., Schwab, U., & Schuchmann, H. P. (2017). Interfacial and emulsifying
800 properties of citrus pectin: Interaction of pH, ionic strength and degree of
801 esterification. *Food Hydrocolloids, 62,* 288-298.

802 Shpigelman, A., Kyomugasho, C., Christiaens, S., Van Loey, A. M., & Hendrickx, M. E.
803 (2014). Thermal and high pressure high temperature processes result in distinctly
804 different pectin non-enzymatic conversions. *Food Hydrocolloids, 39,* 251-263.

805 Singh, H., Ye, A., & Horne, D. (2009). Structuring food emulsions in the gastrointestinal tract
806 to modify lipid digestion. *Progress in Lipid Research, 48,* 92-100.

807 Tokle, T., Mao, Y., & McClements, D. J. (2013). Potential biological fate of emulsion-based
808 delivery systems: Lipid particles nanolaminated with lactoferrin and β-lactoglobulin
809 coatings. *Pharmaceutical Research, 30,* 3200-3213.

810 Tsujita, T., Takaichi, H., Takaku, T., Sawai, T., Yoshida, N., & Hiraki, J. (2007). Inhibition of
811 lipase activities by basic polysaccharide. *Journal of Lipid Research, 48,* 358-365.

812 Verkempinck, S. H. E., Salvia-Trujillo, L., Moens, L. G., Carrillo, C., Van Loey, A. M.,
813 Hendrickx, M. E. et al. (2018a). Kinetic approach to study the relation between *in*
814 *vitro* lipid digestion and carotenoid bioaccessibility in emulsions with different oil
815 unsaturation degree. *Journal of Functional Foods, 41,* 135-147.

816 Verkempinck, S. H. E., Salvia-Trujillo, L., Moens, L. G., Charleer, L., Van Loey, A. M.,
817 Hendrickx, M. E. et al. (2018b). Emulsion stability during gastrointestinal conditions
818 effects lipid digestion kinetics. *Food Chemistry, 246,* 179-191.

819 Verrijssen, T. A. J., Balduyck, L. G., Christiaens, S., Van Loey, A. M., Van Buggenhout, S.,
820 & Hendrickx, M. E. (2014). The effect of pectin concentration and degree of methyl-
821 esterification on the *in vitro* bioaccessibility of β-carotene-enriched emulsions. *Food*
822 *Research International, 57,* 71-78.

823 Verrijssen, T. A. J., Verkempinck, S. H. E., Christiaens, S., Van Loey, A. M., & Hendrickx,
824 M. E. (2015). The effect of pectin on *in vitro* β-carotene bioaccessibility and lipid
825 digestion in low fat emulsions. *Food Hydrocolloids, 49,* 73-81.

826 Willats, W. G. T., McCartney, L., Mackie, W., & Knox, J. P. (2001). Pectin: cell biology and
827 prospects for functional analysis. *Plant Molecular Biology, 47,* 9-27.

828 Zhang, R., Zhang, Z., Zou, L., Xiao, H., Zhang, G., Decker, E. A. et al. (2016). Enhancement
829 of carotenoid bioaccessibility from carrots using excipient emulsions: influence of
830 particle size of digestible lipid droplets. *Food & Function, 7,* 93-103.
831
832

833 **Table 1: Changes on the ζ-potential of the initial emulsion, chyme and digest. Different letters in the same**
834 **column indicate significant differences (Tukey test: $p < 0.05$) among the samples. For interpretation of the**
835 **abbreviations is referred to the abbreviation list.**

	Emulsion		Gastric phase		Small intestinal phase	
TW	-7.84 ± 1.19	BC	-3.18 ± 0.70	AB	-31.15 ± 0.26	ABC
PC	2.43 ± 0.24	A	-1.35 ± 0.29	A	-33.80 ± 1.70	BCD
CP82	-14.05 ± 1.13	D	-5.07 ± 0.25	B	-38.95 ± 2.59	D
CP38	-23.13 ± 0.13	F	-10.00 ± 0.49	C	-33.50 ± 2.69	CD
CP10	-30.95 ± 0.54	G	-15.13 ± 0.59	D	-36.53 ± 2.56	CD
TWCP82	-5.60 ± 0.65	B	-3.34 ± 0.61	AB	-31.05 ± 2.43	ABC
TWCP38	-7.53 ± 0.02	BC	-3.16 ± 0.21	AB	-26.38 ± 1.80	A
TWCP10	-9.59 ± 3.42	C	-3.07 ± 0.24	AB	-28.70 ± 1.56	AB
PCCP82	0.03 ± 0.06	A	-4.08 ± 3.57	AB	-39.10 ± 1.27	D
PCCP38	-19.53 ± 0.42	E	-4.85 ± 0.47	B	-37.68 ± 5.50	D
PCCP10	-23.93 ± 1.06	F	-11.07 ± 1.03	C	-35.37 ± 2.88	CD

836

837

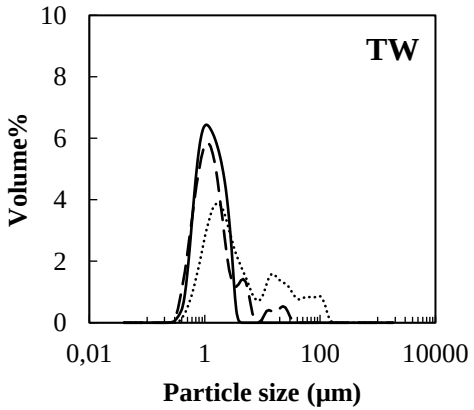

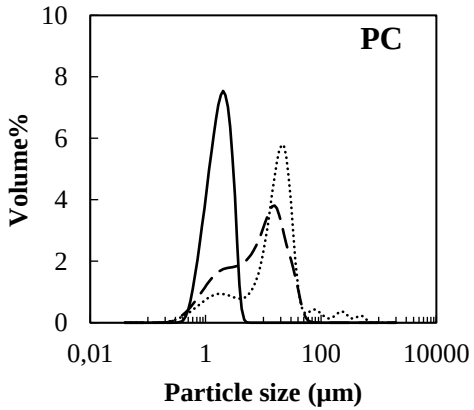

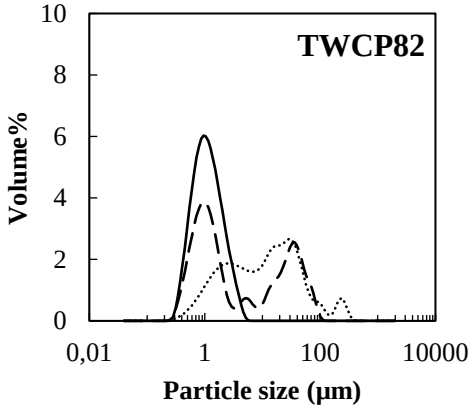

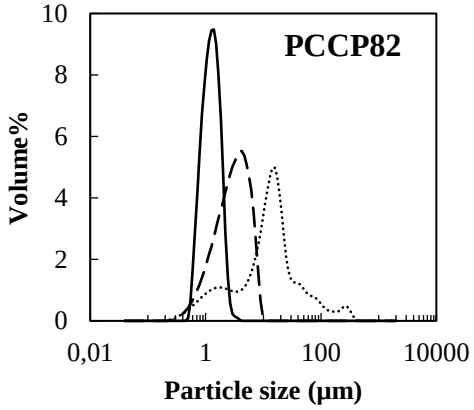

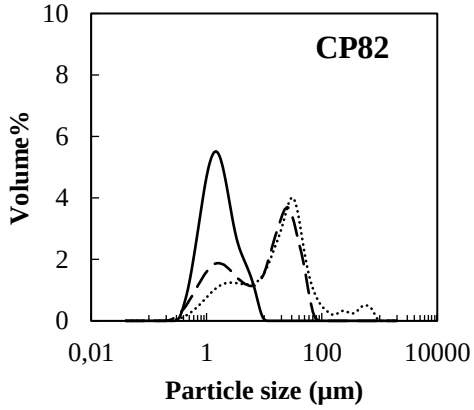

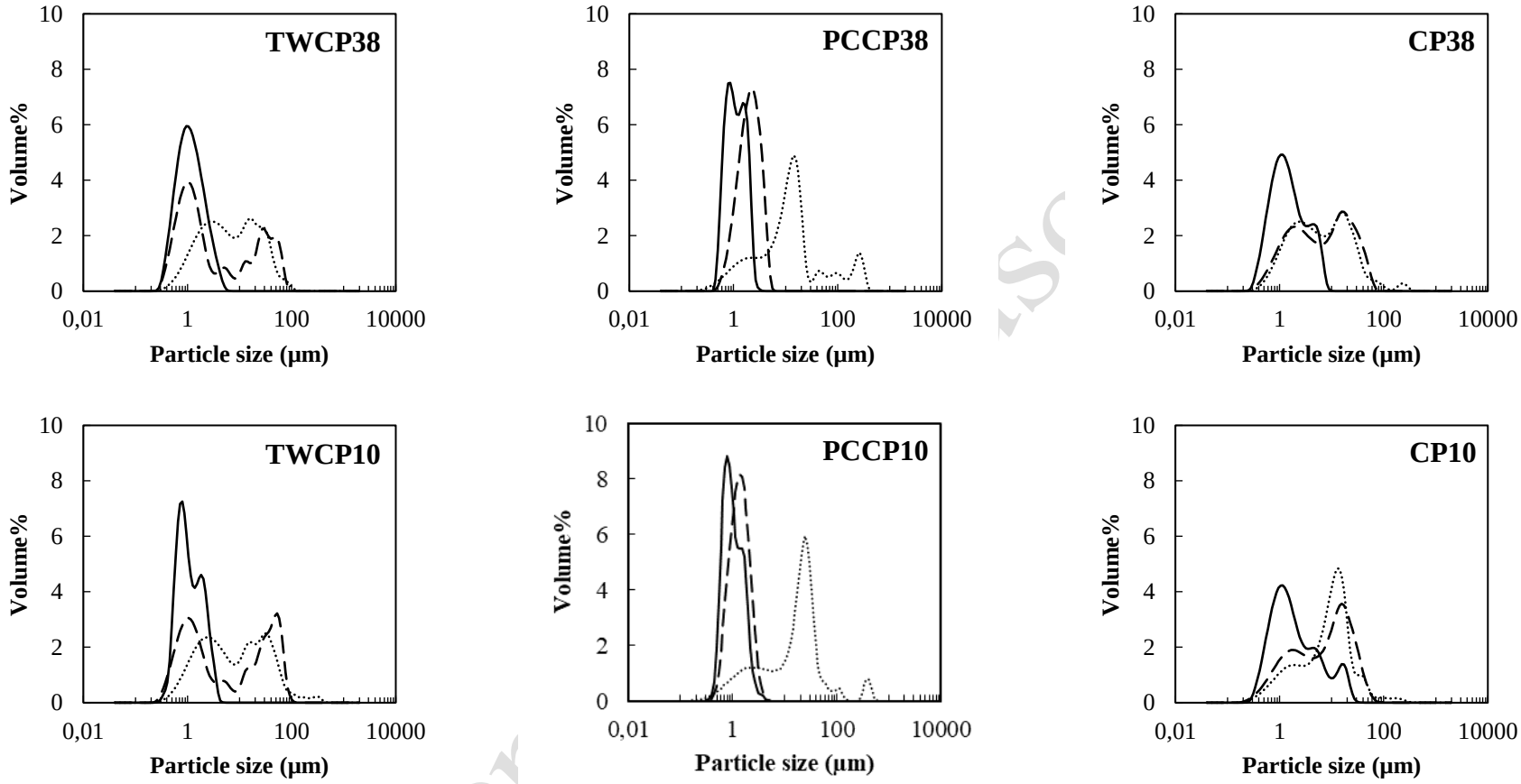

Figure 1: Particle size distribution of all carrot-enriched oil-in-water emulsions during digestion (full line: initial emulsion; dashed line: chyme (2h); dotted line: digest (2h)). For interpretation of the abbreviations is referred to the abbreviation list.

838

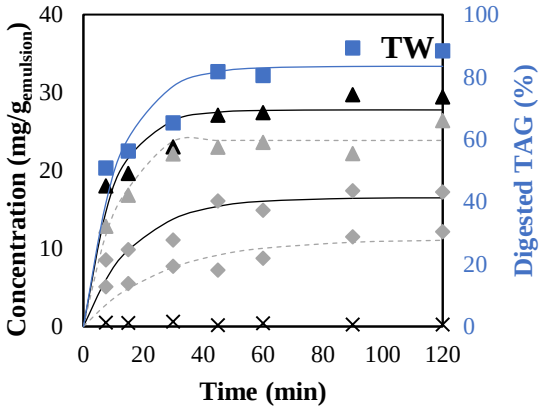

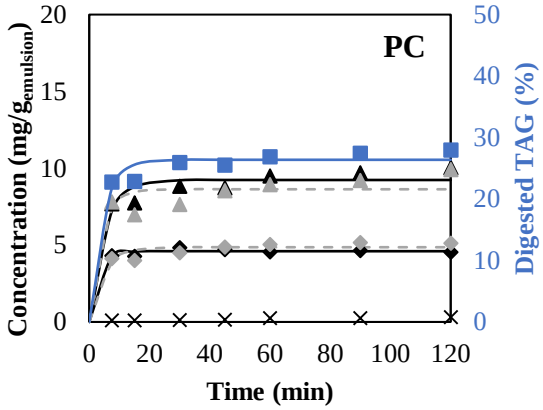

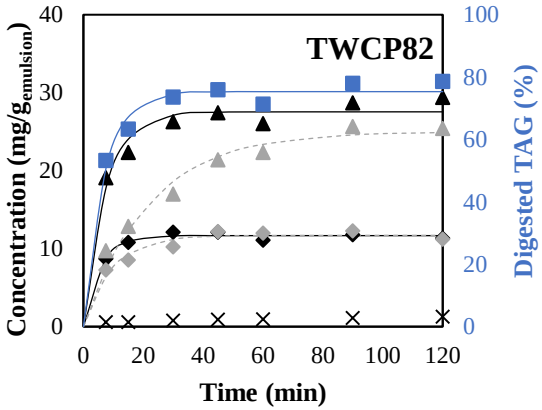

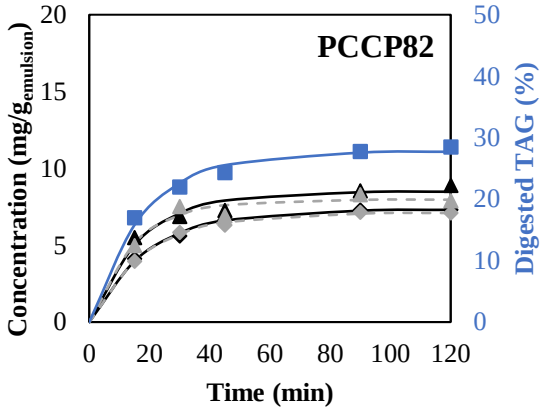

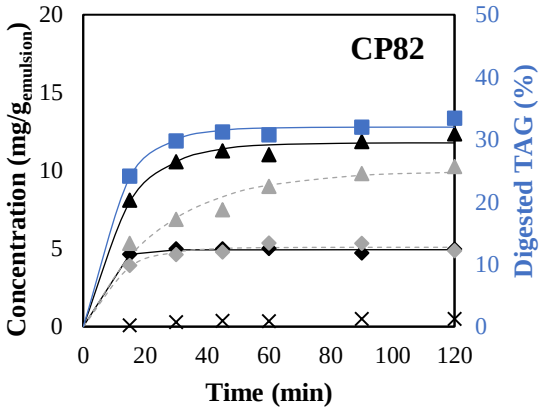

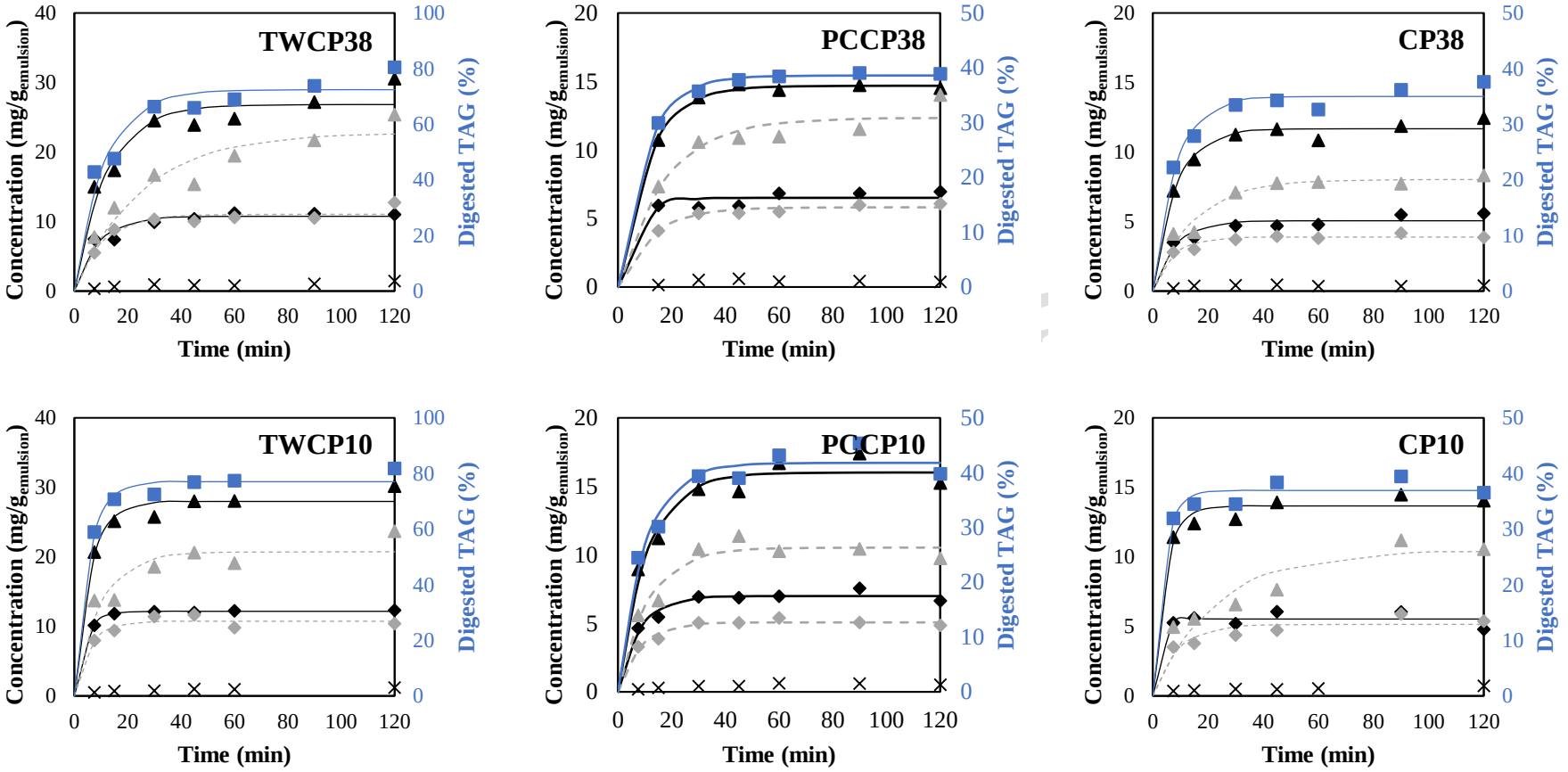

Figure 2: ***In vitro*** **lipid digestion of carrot-based emulsions as function of small intestinal digestion. The symbols indicate the experimental data while the full and dotted lines show the predicted values of the corresponding fractional conversion model in the digest and micellar fraction, respectively (■ TAG_{digest}; ◆ MAG_{digest}; ◆ $MAG_{micelle}$; ▲ FFA_{digest}; ▲ $FFA_{micelle}$; ✕ GLY_{digest}). For representation in color is referred to the online version and for the interpretation of the abbreviations is referred to the abbreviation list.**

839

Table 2: Estimated kinetic parameters of the different carrot-based emulsions modelled by a fractional conversion model through a nonlinear regression procedure. C_f is the final lipid concentration estimated by the model (expressed in % in case of TAG and mg/g emulsion in all other cases) and k is the incorporation rate constant of the lipids into micelles (min^{-1})). For interpretation of the abbreviations is referred to the abbreviation list.

	TAG_{digest}	MAG_{digest}	FFA_{digest}	$MAG_{micelle}$	$FFA_{micelle}$
	TW				
***k* ± stdev**	0.086 ± 0.018	0.060 ± 0.014	0.100 ± 0.020	0.038 ± 0.012	0.090 ± 0.012
C_f ± stdev	83.40 ± 3.93	16.51 ± 1.01	27.77 ± 1.16	11.17 ± 1.16	23.86 ± 0.70
R^2_{adj}	0.923	0.906	0.933	0.851	0.962
	PC				
***k* ± stdev**	0.233 ± 0.045	0.344 ± 0.068	0.203 ± 0.045	0.209 ± 0.049	0.254 ± 0.105
C_f ± stdev	26.38 ± 0.64	4.60 ± 0.07	9.24 ± 0.29	4.86 ± 0.16	8.63 ± 0.41
R^2_{adj}	0.969	0.988	0.950	0.945	0.889
	CP82				
***k* ± stdev**	0.092 ± 0.007	0.188 ± 0.028	0.076 ± 0.007	0.092 ± 0.013	0.040 ± 0.006
C_f ± stdev	31.98 ± 0.43	4.93 ± 0.05	11.78 ± 0.22	5.09 ± 0.12	9.98 ± 0.43
R^2_{adj}	0.994	0.995	0.990	0.980	0.893
	CP38				
***k* ± stdev**	0.121 ± 0.014	0.124 ± 0.025	0.120 ± 0.012	0.139 ± 0.022	0.068 ± 0.010
C_f ± stdev	34.99 ± 0.82	5.06 ± 0.20	11.67 ± 0.23	3.88 ± 0.11	8.02 ± 0.31
R^2_{adj}	0.976	0.934	0.983	0.963	0.958
	CP10				
***k* ± stdev**	0.253 ± 0.049	0.402 ± 0.265	0.223 ± 0.039	0.113 ± 0.030	0.044 ± 0.013
C_f ± stdev	36.94 ± 0.88	5.53 ± 0.22	13.66 ± 0.34	5.14 ± 0.31	10.44 ± 0.98
R^2_{adj}	0.977	0.933	0.976	0.892	0.872
	TWCP82				
***k* ± stdev**	0.148 ± 0.016	0.181 ± 0.017	0.138 ± 0.018	0.104 ± 0.015	0.046 ± 0.006
C_f ± stdev	75.34 ± 1.41	11.67 ± 0.17	27.54 ± 0.67	11.70 ± 0.36	25.00 ± 0.98
R^2_{adj}	0.984	0.989	0.973	0.962	0.973
	TWCP38				
***k* ± stdev**	0.089 ± 0.016	0.112 ± 0.021	0.082 ± 0.016	0.096 ± 0.017	0.040 ± 0.009
C_f ± stdev	72.42 ± 2.90	10.75 ± 0.41	26.83 ± 1.20	11.04 ± 0.42	22.79 ± 1.71
R^2_{adj}	0.943	0.940	0.932	0.947	0.915
	TWCP10				
***k* ± stdev**	0.185 ± 0.021	0.240 ± 0.007	0.169 ± 0.024	0.170 ± 0.033	0.101 ± 0.027
C_f ± stdev	77.03 ± 1.48	12.17 ± 0.05	27.97 ± 0.70	10.74 ± 0.37	20.73 ± 1.28
R^2_{adj}	0.986	0.999	0.977	0.959	0.895
	PCCP82				
***k* ± stdev**	0.056 ± 0.005	0.052 ± 0.002	0.060 ± 0.009	0.054 ± 0.002	0.069 ± 0.012
C_f ± stdev	27.74 ± 0.69	7.32 ± 0.09	8.49 ± 0.31	7.11 ± 0.08	7.97 ± 0.31
R^2_{adj}	0.989	0.997	0.973	0.998	0.968
	PCCP38				
***k* ± stdev**	0.097 ± 0.004	0.147 ± 0.050	0.089 ± 0.004	0.080 ± 0.009	0.057 ± 0.012
C_f ± stdev	38.59 ± 0.24	6.51 ± 0.23	14.69 ± 0.12	5.81 ± 0.12	12.35 ± 0.62
R^2_{adj}	0.999	0.951	0.998	0.987	0.941
	PCCP10				
***k* ± stdev**	0.099 ± 0.013	0.126 ± 0.016	0.091 ± 0.013	0.120 ± 0.014	0.088 ± 0.015
C_f ± stdev	41.78 ± 1.20	6.99 ± 0.17	16.01 ± 0.50	5.07 ± 0.12	10.53 ± 0.39
R^2_{adj}	0.968	0.973	0.964	0.977	0.952

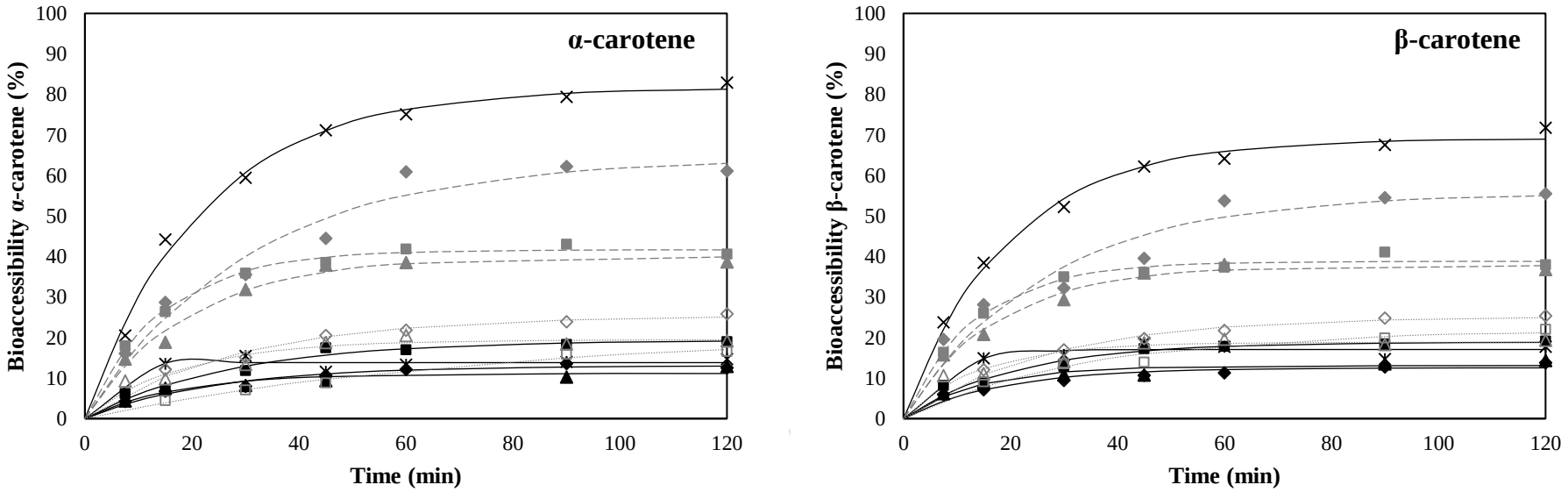

Figure 3: Time dependent evolution as function of small intestinal digestion time of α- and β-carotene. The symbols indicate the experimental data, while the lines show the predicted values of the corresponding fractional conversion model. Full lines represent mono-emulsifier emulsions (✕ TW; ✱ PC; ■ CP82; ◆ CP38 and ▲ CP10); dashed lines represent the tween-pectin emulsions (■ TWCP82; ◆ TWCP38 and ▲ TWCP10) and dotted lines represent the phosphatidylcholine-pectin emulsions (■ PCCP82; ◆ PCCP38 and ▲ PCCP10). For interpretation of the abbreviations is referred to the abbreviation list.

846

Table 3: Estimated kinetic parameters (± standard deviation) of the different carotenoid-enriched emulsions modelled by a fractional conversion model through a nonlinear regression procedure (*k*: incorporation rate constant of carotenoids into micelles and BAC_f: final bioaccessibility estimated by the model). For interpretation of the abbreviations is referred to the abbreviation list.

	α-carotene			β-carotene		
TW						
***k* ± stdev (min^{-1})**	0.045	±	0.003	0.051	±	0.003
BAC_f ± stdev (%)	81.66	±	1.58	69.12	±	1.21
R^2_{adj}	0.993			0.994		
PC						
***k* ± stdev (min^{-1})**	0.283	±	0.491	0.134	±	0.047
BAC_f ± stdev (%)	13.82	±	0.60	17.06	±	0.69
R^2_{adj}	0.922			0.937		
CP82						
***k* ± stdev (min^{-1})**	0.037	±	0.006	0.048	±	0.007
BAC_f ± stdev (%)	19.36	±	0.98	18.87	±	0.85
R^2_{adj}	0.965			0.961		
CP38						
***k* ± stdev (min^{-1})**	0.041	±	0.006	0.056	±	0.010
BAC_f ± stdev (%)	13.05	±	0.60	12.54	±	0.64
R^2_{adj}	0.967			0.940		
CP10						
***k* ± stdev (min^{-1})**	0.058	±	0.014	0.071	±	0.014
BAC_f ± stdev (%)	11.14	±	0.78	13.09	±	0.70
R^2_{adj}	0.905			0.935		
TWCP82						
***k* ± stdev (min^{-1})**	0.069	±	0.004	0.073	±	0.005
BAC_f ± stdev (%)	41.65	±	0.61	38.81	±	0.67
R^2_{adj}	0.994			0.991		
TWCP38						
***k* ± stdev (min^{-1})**	0.032	±	0.005	0.037	±	0.008
BAC_f ± stdev (%)	64.32	±	3.76	55.67	±	3.75
R^2_{adj}	0.962			0.938		
TWCP10						
***k* ± stdev (min^{-1})**	0.052	±	0.006	0.058	±	0.006
BAC_f ± stdev (%)	39.99	±	1.39	37.79	±	1.22
R^2_{adj}	0.982			0.982		
PCCP82						
***k* ± stdev (min^{-1})**	0.013	±	0.003	0.029	±	0.005
BAC_f ± stdev (%)	21.37	±	2.18	21.83	±	1.40
R^2_{adj}	0.984			0.963		
PCCP38						
***k* ± stdev (min^{-1})**	0.035	±	0.004	0.038	±	0.003
BAC_f ± stdev (%)	25.44	±	0.97	25.20	±	0.65
R^2_{adj}	0.981			0.990		
PCCP10						
***k* ± stdev (min^{-1})**	0.055	±	0.011	0.070	±	0.014
BAC_f ± stdev (%)	19.45	±	1.11	18.85	±	0.95
R^2_{adj}	0.926			0.925		

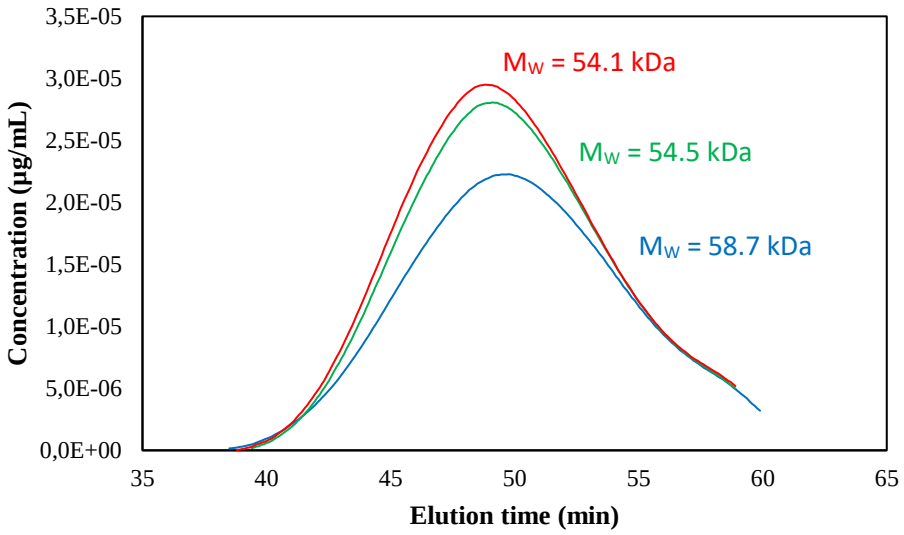

Figure A: Concentration profile and corresponding weight average molecular weight (M_w) of the pectin samples (■ CP82; ◆ CP38 and ▲ CP10).

Table A (supplementary material): Changes on the particle size of the initial emulsion, chyme and digest represented by the median volume-weighted particle size. Different letters in the same column indicate significant differences (Tukey test: $p < 0.05$) among the samples. For interpretation of the abbreviations is referred to the abbreviation list.

	Emulsion		Gastric phase		Small intestinal phase	
TW	1.27 ± 0.10	E	1.29 ± 0.02	E	2.89 ± 0.19	G
PC	1.65 ± 0.01	D	12.71 ± 5.68	A	21.22 ± 4.80	A
CP82	1.42 ± 0.02	B	6.75 ± 0.89	BCD	6.48 ± 1.04	F
CP38	1.67 ± 0.08	A	8.30 ± 0.10	BC	9.99 ± 0.32	DE
CP10	1.12 ± 0.01	F	1.96 ± 0.30	E	11.90 ± 1.71	CD
TWCP82	1.14 ± 0.01	F	1.86 ± 0.08	E	6.70 ± 0.51	F
TWCP38	1.06 ± 0.05	FG	4.33 ± 0.52	CDE	8.01 ± 1.11	EF
TWCP10	1.82 ± 0.07	C	9.78 ± 3.34	AB	17.62 ± 1.44	B
PCCP82	1.30 ± 0.01	E	3.19 ± 0.03	DE	13.52 ± 0.51	C
PCCP38	1.13 ± 0.02	F	2.13 ± 0.01	E	12.11 ± 0.28	CD
PCCP10	1.01 ± 0.03	G	1.41 ± 0.01	E	19.30 ± 0.99	AB

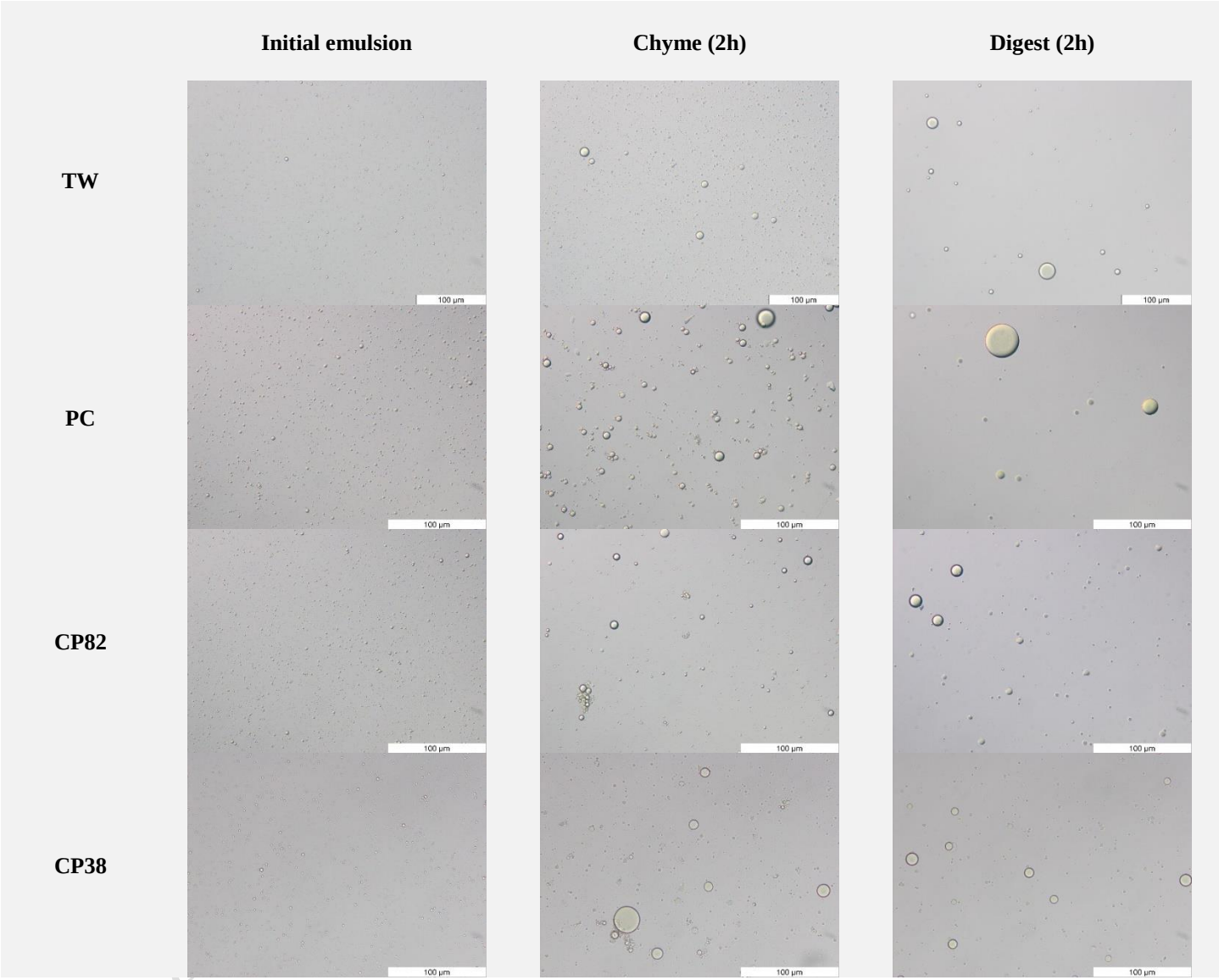
Initial emulsion
Chyme (2h)
Digest (2h)
TW
PC
CP82
CP38
100 µm

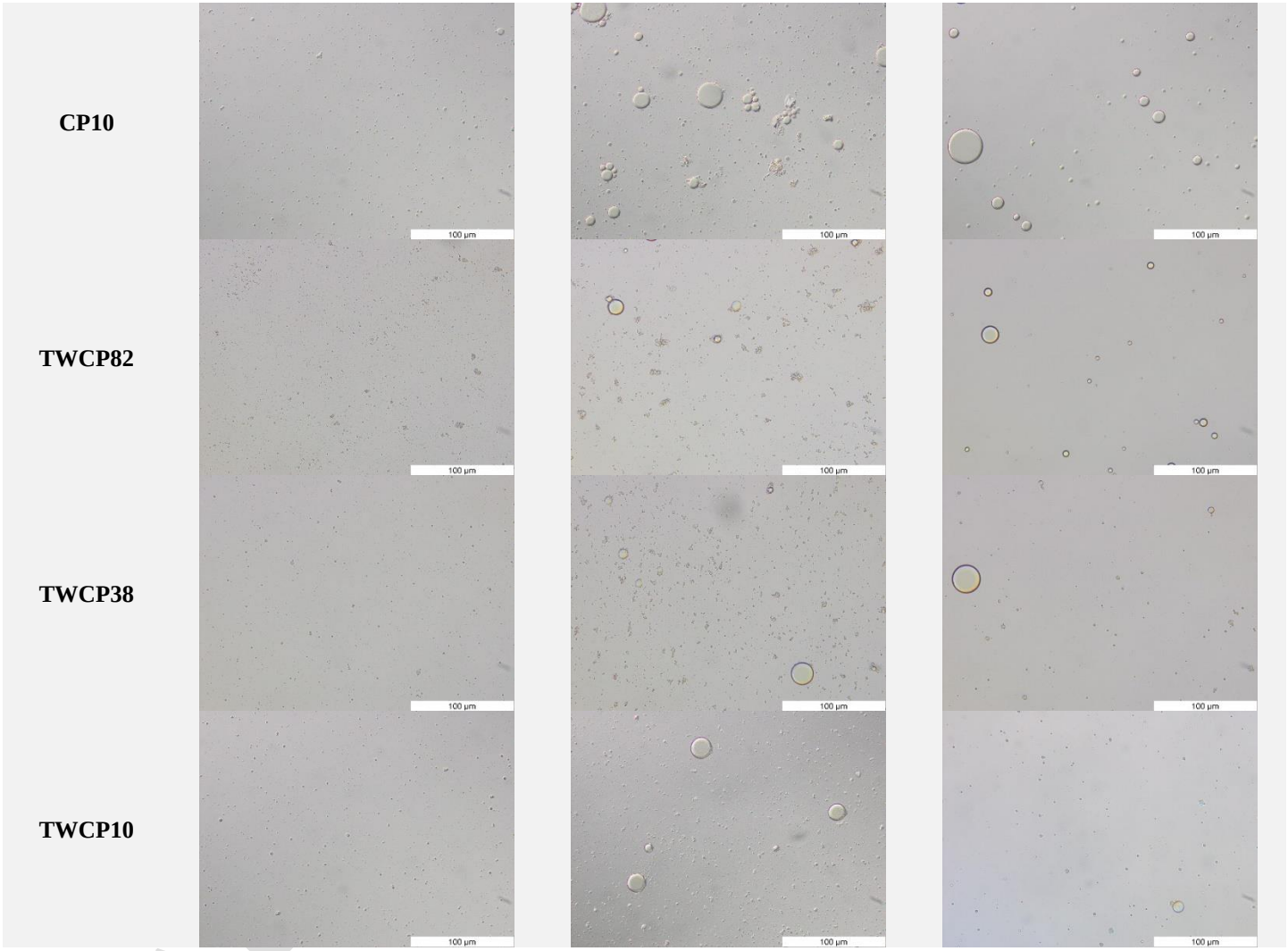
CP10
TWCP82
TWCP38
TWCP10
100 µm

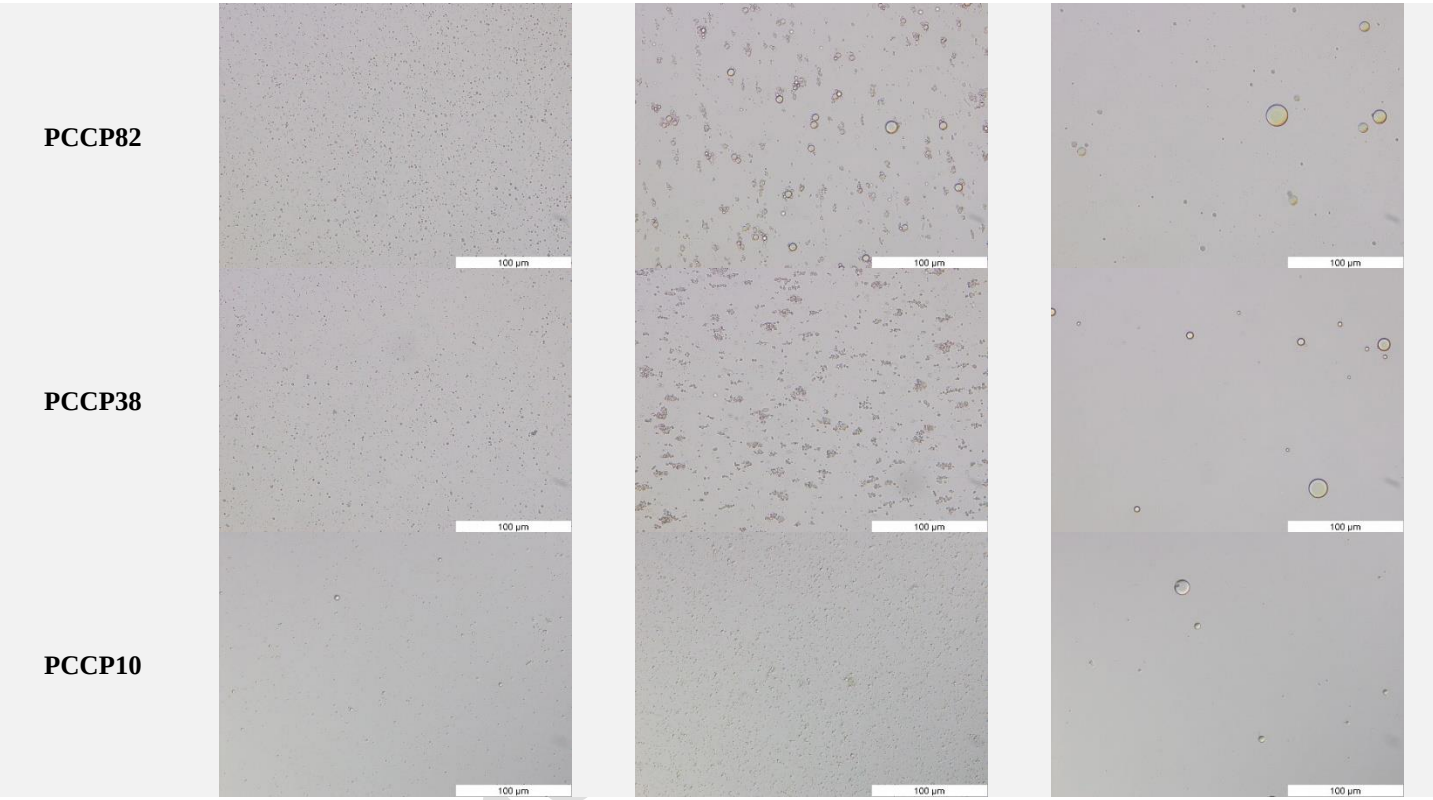

Figure B: Changes in microstructure of all carrot-based oil-in-water emulsions during digestion (scale bar represents a length of 100 µm). For interpretation of the abbreviations is referred to the abbreviation list.

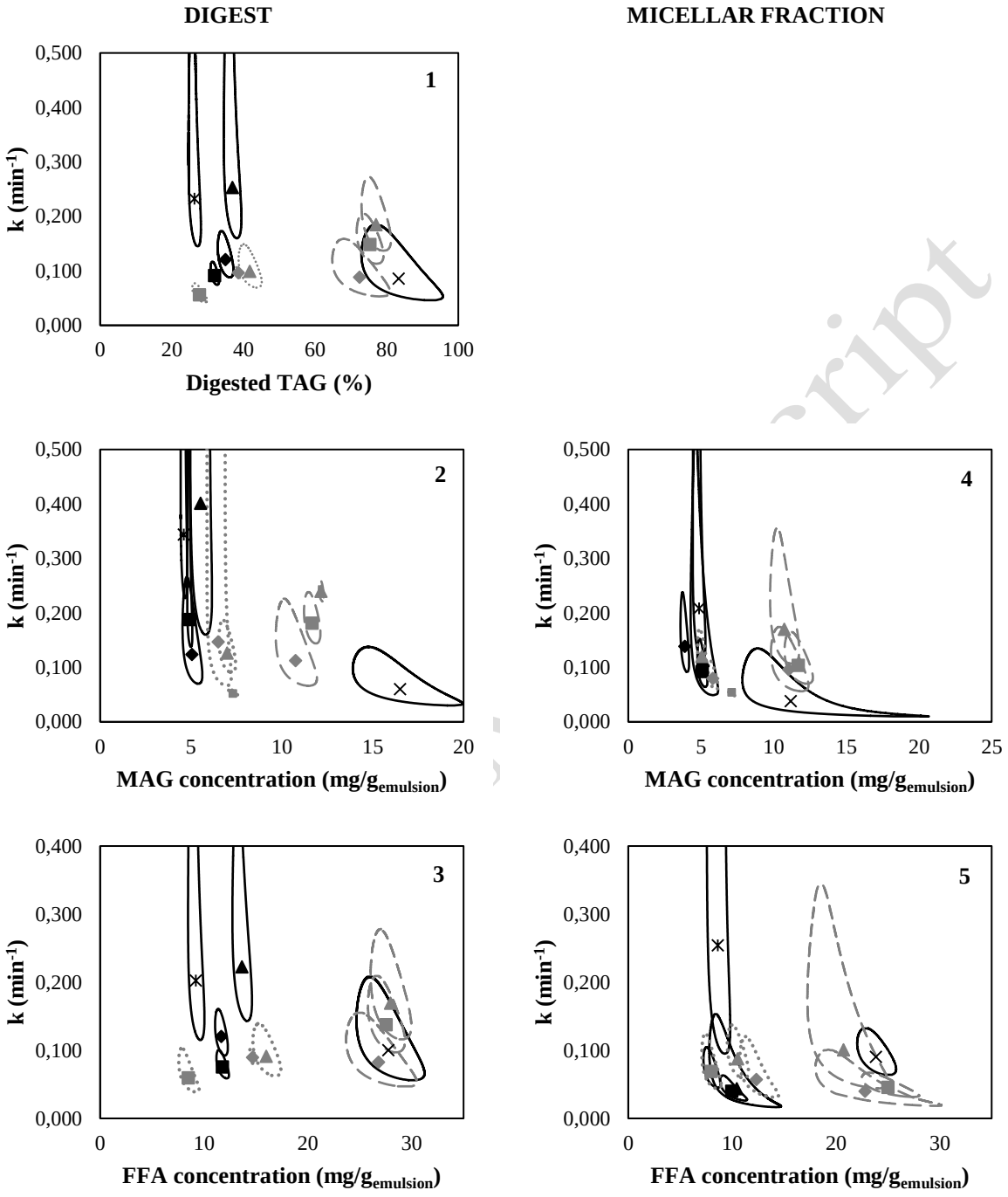

Figure C: Joint confidence region analysis (90%) of the jointly estimated parameters (Table 2) for *in vitro* small intestinal lipid digestion: (1) TAG in the digest; (2) MAG in the digest; (3) FFA in the digest; (4) MAG in the micellar fraction and (5) FFA in the micellar fraction The symbols indicate the estimated value of the corresponding fractional conversion model, while the lines show the joint confidence region. Full lines represent mono-emulsifier emulsions (✕ TW; ✱ PC; ■ CP82; ◆ CP38 and ▲ CP10); dashed lines represent tween-pectin combined emulsions (■ TWCP82; ◆ TWCP38 and ▲ TWCP10) and dotted lines represent phosphatidylcholine-tween combined emulsions (■ PCCP82; ◆ PCCP38 and ▲ PCCP10). For interpretation of the abbreviations is referred to the abbreviation list.

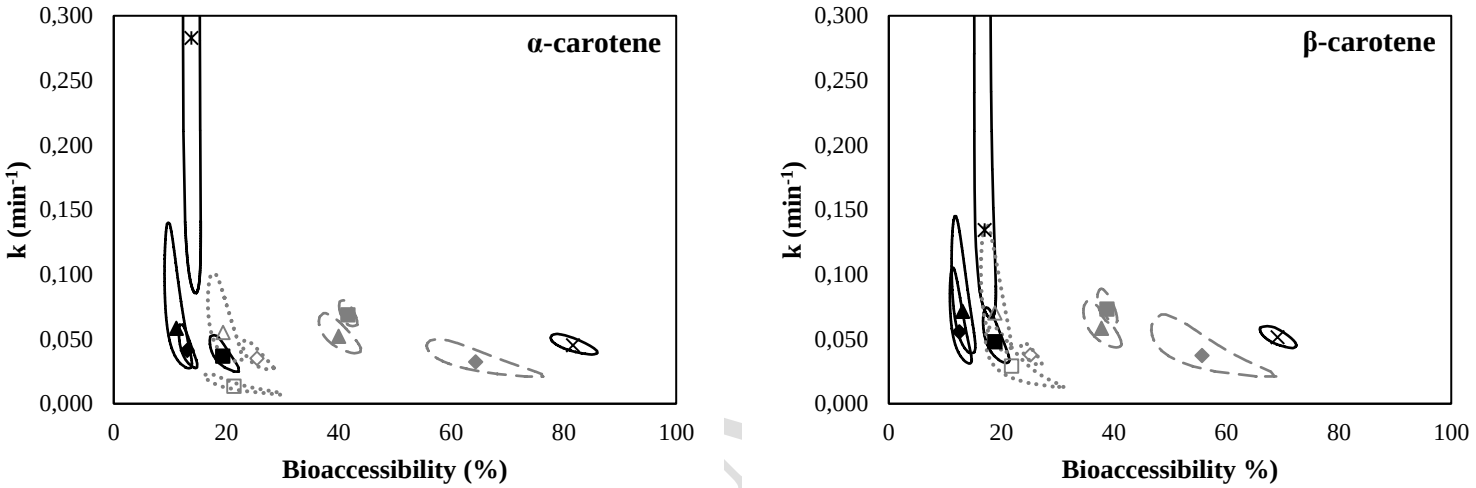

Figure D: Joint confidence region analysis (90%) of the jointly estimated parameters (Table 3) for carotenoid bioaccessibility of α- and β-carotene. The symbols indicate the experimental data, while the lines show the joint confidence region. Full lines represent mono-emulsifier emulsions (✕ TW; ✱ PC; ■ CP82; ◆ CP38 and ▲ CP10); dashed lines represent the tween-pectin emulsions (■ TWCP82; ◆ TWCP38 and ▲ TWCP10) and dotted lines represent the phosphatidylcholine-pectin emulsions (■ PCCP82; ◆ PCCP38 and ▲ PCCP10).

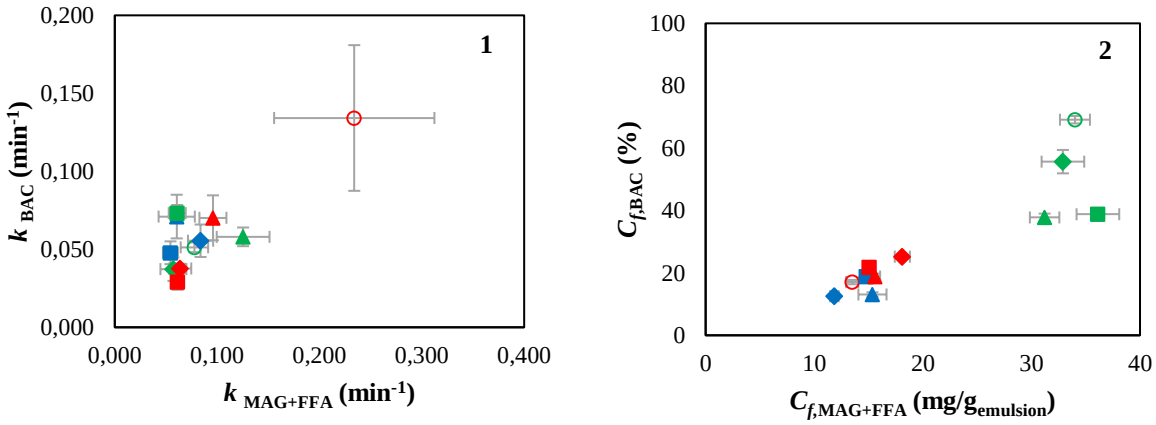

Figure E: Relation between the (1) *k*-values (min^{-1}) and (2) C_f-values of MAG and FFA micellarisation, and carotenoid incorporation into mixed micelles (○ TW; ○ PC; ■ CP82; ◆ CP38; ▲ CP10; ■ TWCP82; ◆ TWCP38; ▲ TWCP10; ■ PCCP82; ◆ PCCP38; ▲ PCCP10). For interpretation of the abbreviations is referred to the abbreviation list.